TECHNISCHE UNIVERSITÄT DRESDEN

**Bereich Mathematik und Naturwissenschaften** Fakultät Physik, Institut für Kern- und Teilchenphysik

Master Thesis

# Comparison of analytical and parton-shower approaches to soft-gluon resummation at NLL accuracy

Daniel Reichelt

Born on: 9th February 1992 in Dresden

Matriculation number: 3810013

Matriculation year: 2011

to achieve the academic degree

Master of Science (M.Sc.)



First referee

Dr. Frank Siegert

Second referee

Prof. Dr. Steffen Schumann

Submitted on: 11th December 2017

This thesis is based on work done in collaboration with Dr. Stefan Höche and Dr. Frank Siegert. The main results are also made public in [1]:

S. Höche, D. Reichelt and F. Siegert,
*Momentum conservation and unitarity in parton showers and NLL resummation*,
`arXiv:1711.03497` [hep-ph],
Submitted to JHEP for publication.

Diese Arbeit basiert auf Zusammenarbeit mit Dr. Stefan Höche und Dr. Frank Siegert. Die Ergebnisse wurden auch in [1] veröffentlicht:

S. Höche, D. Reichelt und F. Siegert,
*Momentum conservation and unitarity in parton showers and NLL resummation*,
`arXiv:1711.03497` [hep-ph],
Eingereicht bei JHEP zur Veröffentlichung.

## Abstract

This thesis presents a systematic study of the differences between analytic soft gluon resummation at next-to-leading logarithmic accuracy and parton shower algorithms. First, the necessary formalisms are briefly reviewed. A Markovian Monte-Carlo algorithm for resummation of additive three-jet observables in electron-positron annihilation to hadrons is constructed and tuned to exactly reproduce the analytic calculation in the CAESAR formalism. The correctness is verified by comparison to analytic results and by explicit investigation of the infrared limit. Three observables, thrust, a BKS observable and a fractional energy correlation, are considered as specific examples. Approximations intrinsic to resummation are then removed, in order to obtain a traditional, momentum and probability conserving parton shower. The impact of each of the different approximations is studied, and an overall comparison is made between parton shower and pure resummation of leading and next-to-leading logarithms. Finally, differences in comparison to modern parton shower algorithms formulated in terms of color dipoles are analysed.

## Zusammenfassung

Diese Arbeit stellt eine systematische Studie der Unterschiede zwischen der analytischen resummation von weichen Gluonen auf nächst führender logarithmischer Genauigkeit und Parton-Shower Algorithmen vor.
Zunächst werden die benötigten Formalismen behandelt. Ein Markovscher Monte-Carlo Algorithmus zur Resummation von additiven drei-Jet Observablen in Elektron-Positron Annihilation zu Hadronen wird konstruiert und angepasst, um genau das analytische resultat des CAESAR-Formalismus zu reproduzieren. Die Korrektheit wird durch direkten Vergleich mit analytischen Ergebnissen und durch explizite Untersuchung des infraroten Limes verifiziert. Drei Observable, Thrust, eine BKS-Observable und eine Teil-Energie-Korrelation, werden als konkrete Beispiele betrachtet.
Der Resummation intrinsische Näherungen werden anschließend entfernt, um letztendlich einen traditionellen, impuls- und wahrscheinlichkeitserhaltenden Parton-Shower zu erhalten. Der Einfluss der jeweiligen Näherungen wird untersucht, und ein Gesamtvergleich zwischen Parton-Shower und reiner Resummation von führenden und nächst führenden Logarithmen wird angestellt. Abschließend werden Unterschiede im Vergleich mit modernen Parton-Shower Algorithmen analysiert, die mithilfe von Farbdipolen formuliert werden.

# Contents

# 1 Introduction

The field of particle physics has seen a rapid progress over the last half century, with a series of experiments, pushing the frontier in accessible energies and amount of data. The experimental developments have been accompanied by huge theoretical efforts to describe the encountered phenomena at ever higher precision.

At the present time, the large hadron collider (LHC) collects increasing amounts of data at unpreceded rates [2], and future projects of hadron- [3] and lepton- [4, 5] colliders are in various stages of planning [6]. This necessitates theoretical predictions with increasing precision, as well as further insights into precision that can be expected from existing calculations and the numerical size of neglected contributions.

Measurements of Standard Model (SM) processes as well as searches for new physics are significantly influenced by backgrounds from quantum chromodynamics (QCD). Predictions that experiments routinely compare their results to are made from huge simulation programs, as for example presented in [7, 8, 9, 10, 11, 12], for a review see [13]. They take into account a large number of effects, starting from a fixed order calculation of cross sections that needs to be integrated over some fiducial phase space, usually done by Monte Carlo methods, to non-perturbative effects such as hadronisation of partons into hadrons, multiple parton interactions in hadron collisions and soft interactions between beam remnants.

Of particular interest are events where large hierarchies between the typical (energy-) scales of important physical effects result in huge corrections to tree level results, see also Section 2.2. These contributions must be resummed to all orders in perturbation theory to reliably predict observable quantities. In the simulation programmes mentioned above, resummation is performed by Markov-Chain Monte Carlo algorithms called parton showers [14]. Resummed predictions are also done in analytic calculations, usually with higher formal accuracy than is achieved in parton showers. Nevertheless, parton showers are quite successful in describing data available from a range of experiments [15]. This work investigates differences between typical parton showers and analytic calculations at an equivalent level of accuracy.

Resummation was first performed for energy-energy correlations in $e^+e^-$ collisions [16, 17, 18], transverse momentum dependent cross sections in Drell-Yan events [19, 20, 21] and $e^+e^-$ hadronic event shapes [22]. Several observables in hadron collisions have also been resummed analytically [23]. Such calculations have been extended to very high precision and used, for example, to extract the strong coupling from experimental data in $e^+e^-$ annihilation to hadrons [24, 25]. Effective field theory methods [26, 27] also contribute to rapid progress in this field. General semi-analytic approaches to the problem have been constructed [28, 29, 30, 31, 32, 33, 34] and automated [35] based on direct QCD resummation. They depend only on universal coefficients and are applicable to different processes and a large class of observables.

While parton shower results and analytic resummed calculations are not identical, they achieve the same formal accuracy in simple cases like the annihilation of $e^+e^-$ to jets. A question of interest in this context is how much of the agreement between parton shower predictions and experimental results can be attributed to additional effects taken into account by showers.

In particular, parton showers are constructed as to implement exact four momentum conservation. While this often involves contributions of higher logarithmic order, or even power suppressed terms (see Section 3.2.1), there is a clear physical motivation to include them. On the other hand and more general, it would be desirable to have a better understanding of the actual numerical differences that can be attributed to formally subleading terms, in particular in the light of open theoretical and phenomenological questions and developments, such as discrimination of quark and gluon jets [36] or work towards showers reaching higher logarithmic accuracy [37].

The aim of this work is to study the (subleading) differences between the two approaches in the simplest setup of additive three-jet observables in $e^+e^-$ annihilations, using the semi-analytic CAESAR formalism [33] as an explicit framework for the analytic resummation. A parton shower is constructed that reproduces the pure next-to-leading logarithmic (NLL, see Section 3.2 for a definition) result in this formalism. Effects beyond NLL accuracy are then included step by step. They broadly correspond to probability conserving (unitarity) effects on one side and momentum conserving effects on the other side. This will eventually recover a standard parton shower based on the DGLAP evolution equations (see Sections 2.6 and 3.1.1).

Modern parton showers are often not formulated in this picture, but rather implement radiation from colour dipoles, as for example in [38, 39, 40], see Section 3.1.2 for details. The standard DGLAP shower constructed here will be compared to an implementation of such a dipole shower based on [14], in order to establish to what extent the result apply for general and more modern parton showers.

Although the effects are only investigated in the simplest setup, it might be argued that many of the results hold for more general approaches. In particular, the effects discussed here will remain if more complicated color structures of the Born configuration are present as this amounts to a multiplicative factor on the distributions shown later. This is for example found in dijet production in hadron-hadron collisions Parton showers would typically only implement the leading color behaviour,[1] although

[1]The leading color approximation here means that terms that are suppressed by factors of $1/N_c^2$, with $N_c$ the number of colours in the theory, are neglected. For the physical case of $N_c = 3$, this means an accuracy at the level of 10% can be expected. The Casimir factors belonging to the representation of particles are however calculated with the physical case $N_c = 3$, see Section 2.2.

extensions to include subleading terms have been published [41, 42].

Higher order resummed calculations, in analytic and numeric approaches, will eliminate part of the effects presented here, which are manifestations of these ambiguities. However, the differences associated with power suppressed corrections, which in the shower are determined by momentum conservation constraints, will remain even if arbitrary higher logarithmic orders are taken into account. In that sense, the results should be taken as systematic uncertainties of the resummation, but also of any approach which leaves out these corrections.

# 2 Theory of the strong interaction

This section collects some general results from perturbation theory of QCD which are needed in the following, for completeness and to set up some notation. First, the theory will be put into context by describing its place in the standard model.

In the subsequent sections, key results relevant for the study presented here will be reviewed and discussed. While the concept of confinement (Section 2.3) is mostly relevant for the discussion and understanding of the applicability of the result, the infrared limit of scattering amplitudes (Section 2.4) is the starting point for resummed calculations, and knowledge of the running of the strong coupling constant (Section 2.2) is crucial to achieve the NLL accuracy discussed here. The concept of (recursive) infrared and collinear safety (Section 2.5) will determine the set of observables to which the formalisms discussed here are applicable. A discussion of the DGLAP equations (Section 2.6) will provide the context for parton shower algorithms. The effects discussed in these sections are standard results of perturbative QCD, and presentations similar to the one given here can be found in many textbooks, see for example [15, 43, 44, 45, 46]

This will introduce most of the formulas needed later, and provide some background for the discussion of the results. The formalisms of parton showers and resummation implemented here, however, are discussed in more detail in the next chapter dedicated to them, as the use of these frameworks is central to the main result of this study.

## 2.1 Quantum chromodynamics as part of the Standard Model

The Standard Model of particle physics is a local quantum field theory, and successfully describes all experiments conducted so far regarding the fundamental components of matter.[1] Except for gravitational observations and the matter-antimatter asymmetry [49], it is believed to describe, at least in principle, all phenomenons observed so far in the universe, although further theoretical arguments may hint to possible extensions [50].

The Standard Model can broadly be separated into an electroweak part, and the theory of QCD. In the low energy regime, QCD is believed to be a confining theory, see Section 2.3, meaning that the fundamental degrees of freedom here are hadrons like protons and neutrons which form most of the matter surrounding us. Electroweak symmetry breaking [51, 52, 53] results in large masses of the W and Z bosons that mediate weak interactions. Thus in the low energy regime electroweak forces are best described by quantum electrodynamics, the theory of photons and electrically charged

[1] There are some anomalies observed in precision observables such as the anomalous magnetic moment of the muon [47] and decays of B mesons [48]. Separately, they are however not statistically significant by the usual standard and it is unclear whether they hint to new physics or will be resolved by future measurements.

particles left over after symmetry breaking, and higher order contact interactions between fermions that stir their weak decay. By that they are important also for the decay of hadrons that would be stable in pure QCD.

At higher energies, above the mass of the Higgs boson discovered at the LHC [54, 55], weak and electrodynamic forces are unified to the above mentioned electroweak interaction. It is described by a $SU(2) \times U(1)$ gauge theory [56, 57, 58].

The degrees of freedom relevant for QCD at these energies are the fermionic quarks which interact via vector mediators called gluons. The essential features are captured in the empirical parton model [59, 60], that describes hadrons as being composed of partons, later to be identified as quarks and gluons, but ignoring much of the microscopic details. While this view is justified in some approximations, fundamentally quarks and gluons are described by operators in the fundamental and adjoint representation of the QCD gauge group $SU(3)$.

The fact that quarks and gluons rather than hadrons are the fundamental degrees of freedom at high energies should be understood in the sense that observables can be calculated in a theory of free quarks and gluons, convoluted with functions that describe their relation to hadrons. Formally, this view is justified by factorization theorems for some processes, such as deep inelastic scattering of a lepton off a proton, the Drell-Yan process, inclusive identified hadron production in lepton collisions and heavy-quark or jet production in hadron collisions [61], see also Section 2.3. The resulting formulas are commonly believed to be at least a good approximation also in processes where the derivation is less rigorous and are taken as a starting point for theory calculations.

In this work, the annihilation of electron-positron pairs into jets is considered, which is at leading order described by the parton level process $e^+e^- \to q\bar{q}$. Corrections due to hadronization are commonly described by phenomenological models in Monte Carlo programs e.g. [62, 63, 64, 65], or by analytic approaches, as for example [66, 67, 68, 69, 70, 71].

Quark masses, except for the top quark, are so low that they can be treated as massless at the energies at which modern experiments, like ATLAS and CMS at the LHC but also lepton colliders like LEP are conducted. Gluons are exactly massless as far as perturbation theory is concerned. This means that parton energies can approach zero. Additionally, matrix elements exhibit singularities when angular distances between partons become arbitrarily small. The limit where this happens is called the infrared limit, and particular attention has to be paid to it, as it leads to divergences in naive higher order calculations.

These divergences are not physical, however. The Kinoshita-Lee-Nauenberg (KLN) theorem [72, 73], an extension of the Bloch-Nordsieck theorem [74] to the full Standard

Model, guarantees that they cancel between virtual corrections for $n$-parton matrix elements and real corrections leading to $n+1$-parton matrix elements. However, the remainder can be large, as will be seen in Section 2.4, necessitating the resummation of these contributions, which is the main focus of this work.

## 2.2 The running coupling constant

QCD is a renormalisable theory. However, as usual, there is no unique renormalisation scheme that dictates the precise procedure how divergences are regularised and absorbed into counterterms. The choice of a renormalisation scheme involves the introduction of an artificial mass scale $\mu$ on which results, obtained at finite order in perturbation theory, depend. Yet, physical results have to be independent of this choice. That leads to renormalization group equations relating results obtained with different choices of $\mu$. As these equations relate terms in different orders in perturbation theory to each other, a suitable choice of renormalization scale generally improves the reliability of the lower order prediction by minimising higher order contributions.

Typically, the preferred choice of renormalization scale is $\mu^2 \approx Q^2$ where $Q^2$ is the typical mass scale of the process in question, for example the center of mass energy for hadron production in lepton collisions, the transverse momentum of a jet, or the mass (or a related observable) of a produced heavy resonance. This happens because higher orders are typically associated with logarithms of the form $\ln \mu^2/Q^2$, which are avoided or minimised by the above choice. If more than one scale is relevant for a process, for example the production of a heavy resonance of mass $M$ associated with the production of a jet with transverse momentum $k_\mathrm{T}$, not all logarithms can be eliminated.

The logarithms can become very large, e.g. at the LHC jets are measured with transverse momenta as low as $k_\mathrm{T} \sim 20$ GeV [75], at a center of mass energy of up to $7-13$ TeV and a partonic center of mass energy typically still of several hundred GeV. The resulting logarithms appear at every order and are large enough to spoil the convergence[2] of the perturbative series. It is in this case necessary to resum these logarithms, i.e. to take into account the logarithmic enhanced terms of all orders.

The dependence of higher orders on $\mu^2$ can be expressed as a dependence of parameters of the theory, like masses (which are ignored here) or the strong coupling constant $\alpha_s = g_s^2/2\pi$ on this scale. Different renormalization schemes lead to different results, though of course to equivalent predictions for physical observables. For the purpose of this work the renormalization scheme will be the so called $\overline{\mathrm{MS}}$ scheme[3] [78], which is

[2]Convergence should here be understood in the usual sense in perturbation theory, i.e. as a rapid decrease of higher order corrections, such that a stable prediction is possible from the first few terms of the asymptotic series [76].

[3]Further physical effects can formally be absorbed into the running of the strong coupling. This will

commonly used in higher order Standard Model calculations. In this scheme, the value of the strong coupling constant is determined by the differential equation:

$$\frac{\partial \alpha_s}{\partial \ln \mu^2} = -\beta_0 \alpha_s^2 - \beta_1 \alpha_s^3 + O(\alpha_s^4) \ . \tag{2.1}$$

where $\beta_0$ and $\beta_1$ can be obtained from the terms divergent in the limit of high momenta (ultraviolet limit, UV) in a suitably regularised higher order calculation, such that a (partial) one-loop calculation is necessary for $\beta_0$, while $\beta_1$ only appears at two-loop accuracy. One obtains [79, 80]:

$$\beta_0 = \frac{11C_A - 2n_f}{12\pi}, \qquad \beta_1 = \frac{17C_A^2 - 5C_A n_f - 3C_F n_f}{24\pi^2} \ . \tag{2.2}$$

The factors $C_A$ and $C_F$ that appear here are the casimirs of the $SU(N_c)$ gauge group of the theory, often and later also in this work referred to as color factors. The group theory result for these is:

$$C_A = N_c = 3, \qquad C_F = \frac{N_c^2 - 1}{2N_c} = \frac{4}{3} \tag{2.3}$$

where the numerical values hold for the physical case in QCD of $N_c = 3$. Note that the normalisation of the colour operators has already been chosen to $T_R = 1/2$ as is conventional. The coefficients also depend on the number of active quark flavours $n_f$. This number should be chosen to take into account all quarks with masses in a range where they constitute a dynamical degree of freedom at the energy scale of interest.

While formulas will be kept general as far as possible, for the purpose of this work it is assumed that there are five nearly massless quarks, while the top quark with a mass of $m_t \approx 173$ GeV [81] is much heavier than the energy scales considered here. Thus the number of active quark flavours can always be fixed to $n_f = 5$. It should however be kept in mind, that for observables at low energies, there are not only corrections from hadronisation to be expected, but also effects of the finite masses of bottom and charm quarks, which are well in the range where perturbative results would hold in the massless theory at $m_b \approx 4.18$ GeV and $m_c \approx 1.28$ GeV [81].

To one loop, meaning without the term proportional to $\beta_1$, Equation (2.1) can be solved to give a relation between the values of $\alpha_s$ at two different scales $\mu$ and $\mu'$:

$$\alpha_s^{1\mathrm{L}}(\mu'^2) = \alpha_s(\mu^2) \frac{1}{1 + \beta_0 \alpha_s(\mu^2) \ln \mu'^2/\mu^2} \ . \tag{2.4}$$

This solution is singular at $\mu' = \Lambda_{1L}^{\mathrm{massless}} = \mu e^{-1/2\alpha_s\beta_0}$, which is known as Landau pole and marks the ultimate breakdown of any perturbative approach. However, already in

lead to the Catani-Marchesini-Webber [77] scheme in Section 3.2.1. This can however be viewed as another NLL term, and the main features of the running are captured by the $\overline{\mathrm{MS}}$ scheme.

the regime where $\alpha_s$ becomes large, e.g. $\alpha_s/2\pi \approx 1$, it is expected that hadronization corrections dominate any phenomenologically relevant result. The two loop equation can not be solved in closed form, however a convenient approximate solution, that is precise enough for all purposes and is used in the following, is of the form

$$\alpha_s(\mu') = \alpha_s^{1\mathrm{L}}(\mu') + \alpha_s^{2\mathrm{L}}(\mu') \tag{2.5}$$

where the one loop part $\alpha_s^{1\mathrm{L}}(\mu'^2)$ is as given above, and the two loop part is again proportional to the one loop part,

$$\alpha_s^{2\mathrm{L}}(\mu'^2) = \alpha_s^2(\mu^2)\frac{\beta_1}{\beta_0}\frac{\ln\left(1+\beta_0\alpha_s(\mu^2)\ln\mu'^2/\mu^2\right)}{\left(1+\beta_0\alpha_s(\mu^2)\ln\mu'^2/\mu^2\right)^2} \ . \tag{2.6}$$

It can be seen now explicitly that the second term in Equation (2.5) is of higher order in $\alpha_s(\mu^2)$. Thus, in the resummation it will correspond to a NLL correction. Terms of even higher order are not needed for the logarithmic accuracy discussed here. The value of $\alpha_s$ is typically quoted at an energy scale corresponding to the pole mass of the Z boson $M_Z \approx 91.2$ GeV. For the purpose of this work, it will be set[4] to

$$\alpha_s\left((91.2\ \mathrm{GeV})^2\right) = 0.118 \ . \tag{2.7}$$

As detailed before, in the main part of this study, the effect of finite quark masses above the Landau pole will be neglected. They have accordingly be ignored so far in the discussion. The difference between running at one loop and two-loop running as well as calculations including the heavy quark masses are illustrated in Figure 2.1.

The masses of heavy quarks are here taken into account, for the purpose of generating Figure 2.1, by considering the theory with $n_F = 5$ active flavours above the bottom mass of $m_b = 4.18$ GeV, then $n_F = 4$ for $m_c < \mu < m_b$ and $n_F = 3$ below the charm mass of $m_c = 1.28$ GeV. Figure 2.1 also highlights the position of $\mu = 500$ MeV which will later be used as a cutoff in the shower variants where this is necessary. It can be seen that in the completely massless theories the Landau pole is at significantly lower values, as $\alpha_s$ grows much faster for low $\mu^2$. Correspondingly, the value of $\Lambda$ here is somewhat lower than what is typically given in the literature [15] as to be used for phenomenology, where $\Lambda \approx 100 - 400$ MeV is usually quoted.

## 2.3 Confinement and asymptotic freedom

As seen in the previous section, the strong coupling constant, as defined in perturbation theory, formally diverges at small energies. This corresponds to a breakdown of the

[4]The parameters of the Z mass are known with extreme high precision from LEP measurements [82]. Also the value of the strong coupling is known with good precision form different measurements, for example at Hera [83] and LEP [84, 85, 24] as well as from theoretical inputs, e.g. in [86], which can be averaged for best precision [81]. However, for the purpose of this work, which is to quantify systematic differences between the two resummation approaches, it suffices to work with $\alpha_s(Q^2) = 0.118$, which corresponds to $Q^2 \approx M_Z^2$ although this has limited meaning in pure QCD.

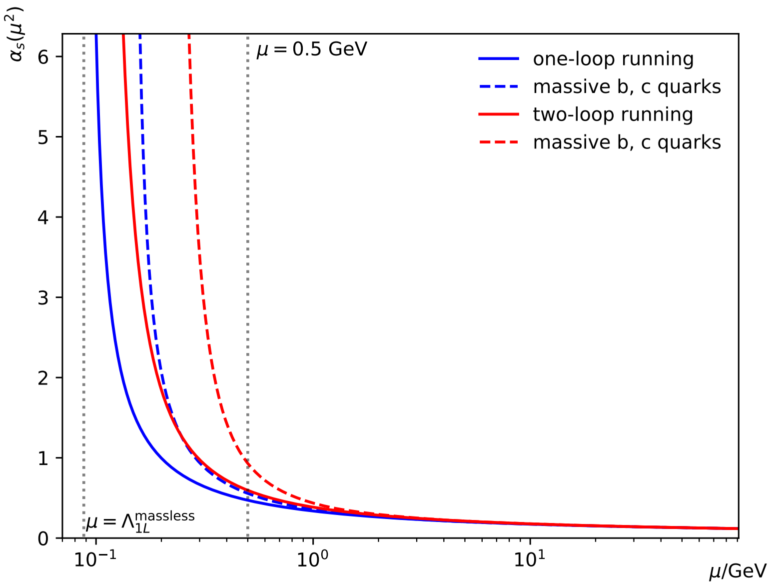


Figure 2.1: Value of the strong coupling constant $\alpha_s$ at different energy scales $\mu$, with $\alpha_s\left((91.2 \text{ GeV})^2\right) = 0.118$. Shown is the running using one and two loop calculations, and calculations including the masses of bottom and charm quarks. The dotted lines mark the position of the Landau pole that is found at one loop in the massless calculation and the point where $\mu = 500$ MeV that is used later as a cutoff.

perturbative approach used to calculate the running. It is generally believed, supported by evidence from numerical results in lattice QCD [87, 88, 89], that QCD is a confining theory. Loosely speaking, this means that the particles accessible in experiments are not the quarks and gluons, but rather hadrons, which can in some sense can be understood as bound states of quarks and gluons.

On the other side, in the limit of very high energies, $Q \gtrapprox 1$ GeV, the strong coupling constant becomes small, and eventually approaches zero in the limit of infinite energies. This behaviour is opposite to that for example found in quantum electrodynamics, and is due to the signs of the $\beta$-coefficients in Equation (2.1), as was noticed in [79, 80]. The smallness of $\alpha_s$ in the regime of high energies justifies the perturbative approach to calculate scattering amplitudes in this region. Formally, this is done by the virtue of so called factorisation theorems, which take the form

$$\frac{d\sigma_{\text{hadron}}}{ds} = \int dx_1\, dx_2\, f(x_1) f(x_2) \frac{d\sigma_{\text{parton}}}{d\hat{s}} \delta(\hat{s} - x_1 x_2 s) \ . \tag{2.8}$$

That is, the hadronic cross section can be written as the convolution of a partonic cross section convolved with distribution functions $f_1$ and $f_2$.

In the case of hadron-hadron collision, for example the Drell-Yan process $pp \to Z$ or the production of the Higgs boson at the LHC by gluon fusion, $f_{1,2}$ describes the internal structure of the incoming protons, or more generally hadrons. At leading order, they can be interpreted as giving the probability distribution to find a quark of some flavour or a gluon in the proton, hence $f$ is called parton distribution function. Similar equations hold for the identified production of hadrons in lepton collisions, where the leading order interpretation is the probability for a parton to fragment into some kind of hadron. Accordingly the functions are called fragmentation functions.

## 2.4 Infrared limit of scattering amplitudes

As already mentioned earlier, the resummation of infrared logarithms handled here is concerned with large contributions from collinear limits of matrix elements. In this limit, the $n$-parton matrix elements $|\mathcal{M}(1,\ldots,n)|^2$ factorises in the following way, with $i$ and $j$ denoting the partons becoming collinear

$$\begin{aligned} d\Phi_{n+1}\,|\mathcal{M}_{n+1}(1,..,i,..,j,..,n)|^2 \approx\, & d\Phi_n\,|\mathcal{M}_n(1,..,ij,..,n)|^2 \\ & \times \frac{dk_\mathrm{T}^2}{k_\mathrm{T}^2}\,dz\,\frac{d\phi}{2\pi}\,\frac{\alpha_s}{2\pi}P_{ij\,i}(z)\ . \end{aligned} \tag{2.9}$$

In this context, $d\Phi_n$ is the $n$-particle phase space element, and $P_{ij\,i}(z)$ is the Altarelli-Parisi splitting kernel associated with the branching of an intermediate parton $ij$ into partons $i$ and $j$. The splitting is characterised by the transverse momentum $k_\mathrm{T}$ relative to the emitting particle and the light cone momentum fraction $z$ in direction of the emitter. The splitting kernels depend on the flavour of the partons involved. For the main part of this study, the only relevant splitting kernel will be the quark-to-quark transition:

$$P_{qq}(z) = C_F\left[\frac{2}{1-z} - (1+z)\right]\ . \tag{2.10}$$

All splitting kernels discussed in this work will be averaged over the polarisations of the particles. The other possibilities are the quark-to-gluon transition, which is related to the above by $z \to 1-z$,

$$P_{qg}(z) = C_F\left[\frac{2}{z} - 2 + z\right] \tag{2.11}$$

and the gluon-to-gluon and gluon-to-quark transitions

$$P_{gg} = C_A\left[\frac{z}{1-z} + \frac{1-z}{z} + z(1-z)\right] \tag{2.12}$$

$$P_{gq} = T_R\left[z^2 + (1-z)^2\right]\ . \tag{2.13}$$

It should be noted that the gluon-to-gluon kernel is symmetric under $z \to 1 - z$, which can be used to map the singularity at $z \to 0$ to the one at $z \to 1$ if integrated over a range symmetric to $z = 1/2$. In this work, the integration range is not symmetric but extended to $z = 0$. A more careful analysis [90], applicable also to higher orders, reveals that the above treatment still gives the correct leading result. Treating the $g \to gg$ splitting function is this way reproduces the correct NLL result in the CAESAR formalism. It can also be seen that $P_{gq}$ does not exhibit any soft singularities associated with $z \to 1$ or $z \to 0$, indicating that it is only present at the level of NLL computations as an addition to the gluon anomalous dimension.

The singularities arising when $z \to 1$ correspond to the emission of a soft particle. The terms later arising from these contributions $\propto 1/(1-z)$ are hence referred to as soft terms, while the remainder, which is proportional to $1 + z$ in the $q \to qg$ case, is called collinear term.

## 2.5 Infrared safety and consistent definition of observables

There are certain conditions observables suitable to be considered here have to meet. This is on one side to ensure basic consistency in their definition as observables in perturbative QCD, in particular that they should be rigorously defined for parton as well as for hadron final states as functions of the four momenta involved, $V(\{p\}, \{k\})$. It is already anticipated in the argument of $V$ that later momenta will be classified as either hard momenta $p$ or soft momenta $k$. There are further limitations resulting from applicability conditions of the CAESAR formalism. In any case, the work here will be limited to rather simple observables, in order to avoid issues related to many coloured legs at Born level.

To ensure that an observable can be calculated in QCD perturbation theory, it is required to be infrared-collinear safe (IRC safe, sometimes in the following referred to as infrared safe), to ensure that it is not very sensitive to the details of physics at low energy scales. This means that is should not change if

- an arbitrary soft four momentum $k_{\text{soft}}$ is removed.
- two collinear momenta $k_1$ and $k_2$ are combined into $k = k_1 + k_2$.

Here, for a four momentum to be soft should be understood to mean that for some reference momentum $p$,

$$k_{\text{soft}} = \lambda p, \qquad \lambda \to 0, \tag{2.14}$$

whereas $k_i$ and $k_j$ are called collinear if, recalling that all four-momenta are assumed to be massless,

$$k_i \cdot k_j \to 0 \ . \tag{2.15}$$

Many observables have been constructed specifically to be infrared safe. A particular class are jet algorithms, that cluster objects in a final state into objects called jets in an infrared safe way. By that, they can be run over hadronic final states, which are experimental accessible, and partonic final states, that are (relatively) easy to calculate from perturbation theory. Assuming local parton-hadron duality [91], observables calculated from these objects, can then be compared to hadronic final states measured in experiments, at least approximately.

In the CAESAR formalism, resummation is carried out for $(n+1)$-jet observables, meaning that that the observable vanishes in the presence of only $n$ particles and behaves in the presence of $n$ hard four momenta and one soft momentum $k$ as a function of only the soft momentum. In this work, the situation considered will always correspond to $n = 2$, and the soft momentum can be parametrised, following the notation of [33] as

$$k = z_1 p_1 + z_2 p_2 + k_\mathrm{T}, \qquad k_\mathrm{T} = 2 p_1 \cdot p_2 z_1 z_2 \tag{2.16}$$

With the rapidity with respect to the emitting $q\bar{q}$ dipole $\eta = 1/2 \ln z_1/z_2$, suitable observables approach zero in the limit where the emitted gluon becomes soft or collinear to the hard particle $l$ as[5] [33]

$$V(\{p\}, k) = V(k) = \left(\frac{k_{T,l}}{Q}\right)^a e^{-b_l \eta_l} \ . \tag{2.17}$$

In general, there can be a normalisation factor $d_l$. For all observables chosen here, it will be $d_l = 1$. If more than two coloured legs are present at the Born level, there can be a factor $g_l(\Phi)$ depending on the azimuthal angle $\Phi$. In the here considered case of only two hard legs, however, the dependence with respect to all legs must be equal, $b_l = b$ and $d_l = d$, and one can use $\eta = \eta_l$, $k_{\mathrm{T},l} = k_\mathrm{T}$ to simplify the notation, as rapidity and transverse momentum with respect to both legs are equal up to a sign. Also, even in the general case the power of the transverse momentum $a$ has to be the same for all legs in the CAESAR formalism, which is already made explicit.

The requirement of recursive infrared collinear safety demands, in contrast to the conditions of usual IRC safety that the behaviour of the observable in the soft limit

[5] This is a further requirement on the observable. It holds however for the observables considered here, and even for a much larger class of observables, see [92].

should not change if further soft particles are added or removed, i.e. when all four momenta $k_i$ involved are soft and/or collinear to one of the hard momenta $p_i$, then the addition of further soft and collinear momenta must not change the observable significantly.

The last requirement is not respected by many popular jet algorithms [33]. For this reason, the so called Durham jet algorithm is the only algorithm that is commonly used in experiments at lepton colliders and is at the same time accessible to study in the CAESAR formalism, for example by studying the jet resolution scales $y_{23}$ corresponding to the scale at which a third jet is resolved. This does however not represent an additive observable, i.e. one that is expressible as the sum over individual soft gluon contributions in the soft limit, to which this study is restricted. It will thus not be further considered.

### Definition of observables

The analysis carried out here will focus on three examples of two-jet observables in $e^+e^-$ annihilation. The definitions are given and discussed below. The coefficients necessary in Equation (2.17) are summarised in Table 2.1. It is well known that these observables fulfil the requirements discussed in the previous section. This and the coefficients in Table 2.1 can be tested and obtained, even for many more observables in more complicated configurations, in an automated fashion in the CAESAR framework. The result for commonly used observables have been made public in [92].

The thrust observable $1-T$ was resummed in [93]. It is defined in terms of final state three-momenta $q_i$ by [94],

$$T = \max_{\vec{n}} \frac{\sum_i |\vec{q}_i \vec{n}|}{\sum_i |\vec{q}_i|} \; . \tag{2.18}$$

The unit vector resulting from the maximisation is called thrust axis $\vec{n}_{\mathrm{T}}$. The resummation is carried out for the observable $1-T$, as this is approaching zero in the two-jet limit. It is a commonly studied observable, at lepton colliders, for example [95, 96, 97, 98].

The BKS observable, a measure of energy flow between jets, was defined, and a resummed calculation provided, in [99, 100] as

$$\mathrm{B}KS_x = \frac{\sum_i E_i |\sin\theta_i|^x (1-|\cos\theta_i|)^{1-x}}{\sum_i |\vec{q}_i|} \; . \tag{2.19}$$

Here the $\theta_i$ are the angles of the momenta with respect to the thrust axis. In the results shown later, the case $x = 1/2$ is considered.

| Observable | $a$ | $b$ | $V(k)$ |
|---|---|---|---|
| Thrust | 1 | 1 | $\frac{k_\mathrm{T}^2/Q^2}{1-z}$ |
| $\mathrm{BKS}_{1/2}$ | 1 | 1/2 | $\sqrt{\frac{k_\mathrm{T}/Q}{1-z}}$ |
| $\mathrm{FC}_1$ | 1 | 0 | $k_\mathrm{T}/Q$ |

Table 2.1: Coefficients in Equation (2.17) to parameterise the observables considered in this work in the soft limit. See also [33, 92]. The last line shows the parametrisation in terms of the transverse momentum with respect to the emitting dipole $k_\mathrm{T}$ and the light cone momentum fraction in direction of the emitter, $z$.

The fractional energy correlation is similar the the BKS observables, however the range of allowed $x$ values can smoothly be extended up to and beyond $x = 1$. It is defined as [33]

$$\mathrm{F}C_x = \sum_{i\neq j} \frac{E_i E_j |\sin\theta_{ij}|^x (1 - |\cos\theta_{ij}|)^{1-x}}{(\sum_i E_i)^2} \Theta\big((\vec{q}_i \vec{n}_T)(\vec{q}_j \vec{n}_T)\big) \ , \tag{2.20}$$

where $\vec{n}_T$ is the thrust axis. The case studied here is $x = 1$. For this choice, it turns out that $b = 0$ and $a = 1$, see Table 2.1. Therefore it scales like $k_\mathrm{T}^2$ in the infrared limit. As this is the evolution variable used in many modern parton showers employed in full simulations for experiments [38, 39, 101], the relation between this observable in the shower and in the analytic calculation is thus particularly simple, reflected by the simple form of the evolution variable chosen later, see section 3.1.1. The same would be true for the three jet resolution scale in the Durham algorithm that would scale as $k_\mathrm{T}^2$ itself. This is however not discussed here, as explained above.

## 2.6 The DGLAP equations

The parton distribution functions and the fragmentation functions in Section 2.3 represent an in principle unphysical separation of effects into a perturbative and a non-perturbative part. In analogy to the renormalization, this leads to an artificial mass scale where the functions are initially fixed at.

Since physical results can not depend on this mass scale, or more generally on the details how the perturbative-non-perturbative separation is performed, this leads to equations analogous to the renormalization group equations that lead to the running coupling in equation 2.1. They are the so called Dokshitzer-Gribov-Lipatov-Altarelli-

Parisi (DGLAP) equations [102, 103, 104, 105],

$$\frac{\partial f_i(x,t)}{\partial \ln t} = \sum_j \int_x^1 \frac{dz}{z}\frac{\alpha_s}{2\pi}\left[P_{ji}\left(z\right)\right]_+ f_j(x/z,t)\ . \tag{2.21}$$

The DGLAP equations as presented here are valid for fragmentation functions $f_i$. In principle they depend on the type of hadron, which is however omitted in the notation as no explicit form of the fragmentation functions is needed. For parton distribution functions, there would be a replacement $\hat{P}_{ji} \to \hat{P}_{ij}$. This corresponds to the physical interpretation of the DGLAP equations, the change of the fragmentation functions happens due to the emission of a collinear parton.

For the case of $P_{qq}$, the function appearing is really a pure plus distribution as denoted in (3.1), for other splitting functions, only part of the function, or none at all, needs to be regularised in this way. The plus distribution can be defined

$$\left[P\left(z\right)\right]_+ = \lim_{\epsilon\to 0}\left[P(z)\Theta(1-z-\epsilon) - \delta(1-z-\epsilon)\int_0^{1-\epsilon} dx\, P(x)\right]\ , \tag{2.22}$$

which ensures that the integral $\int_0^1 dz\left[P\left(z\right)\right]_+ f(z)$ is finite for any test function $f(z)$. In particular, it has the property that $\int_0^1 dz\left[P(z)\right]_+ = 0$. It can be interpreted as the real emission probability plus an endpoint subtraction that corresponds to the virtual contribution cancelling the unresolved real emissions and thus rendering the divergent function finite.

Writing the DGLAP equations out using this, for small but finite $\epsilon$, one arrives at

$$\frac{\partial f_i(x,t)}{\partial \ln t} = \sum_j \int_x^{1-\epsilon} \frac{dz}{z}\frac{\alpha_s}{2\pi}P_{ji}(z)f_j(x/z,t) - f_j(x,t)\int_0^{1-\epsilon} dz\,\frac{\alpha_s}{2\pi}P_{ji}(z) \tag{2.23}$$

Here the strict $\epsilon \to 0$ limit is ignored for a moment, keeping in mind that the $z$ integral will not be extended up to 1 later to ensure momentum conservation in the shower, and that the precise limits are to some extent ambiguous at NLL.

# 3 Resummation of large infrared logarithms

As discussed in the previous section, radiative corrections in QCD perturbation theory must be resummed to all orders to give a sensible description of observables, suitable for comparison to experimental results. There are several approaches, including effective field theory methods, semi-analytic approaches and numerical implementations in so the here discussed parton shower Monte Carlo algorithms.

In this chapter, the principle of parton showers will be described. Further, the analytic CAESAR formalism, introduced in [33], will be reviewed with the parton shower prescription as a starting point. As the main part of this work is concerned only with the rather simple setup of two jet observables in the $e^+e^- \to q\bar{q}$ process, this semi-analytic approach will only be developed as far as necessary for this. For the shower, first a simplified version will be presented, which is sufficient to reproduce the pure NLL result.

Differences to other, more contemporary parton showers, will be outlined and the algorithm used for the comparison to them in Section 5.2 will be introduced. Following, a common framework useful to analyse the differences between the analytical and numerical approaches will be setup, casting the simple parton shower and the CAESAR formalism into a similar language.

## 3.1 Parton showers

The formalism necessary for parton showers will be presented in this section, mostly in a simplified setup. In particular it will be restricted to emissions of gluons from quark lines. This is sufficient to achieve NLL accuracy in the simple two-jet observables in $e^+e^- \to q\bar{q}$, as will be argued in Section 3.2. The same algorithm is in principle capable of reproducing resummed results starting from a colour singlet gluon-gluon final state, with trivial modifications.[1] The formulas needed for the general case will be give in Section 3.1.2 for completeness, together with details on the more recently developed showers, to which the final result of the full shower developed here is compared.

### 3.1.1 Simplified shower

Final state parton showers solve the DGLAP equation, as it was introduced in Section 2.6. For the case considered in this section, where only one type of splitting is considered, it reads:

$$\frac{\partial f_i(x,t)}{\partial \ln t} = \int_x^1 \frac{dz}{z} \frac{\alpha_s}{2\pi} \left[P_{ji}(z)\right]_+ f_j(x/z,t) \; . \tag{3.1}$$

[1] At the level of NLL calculations of three-jet observables considered here, the only difference are the Casimirs, i.e. one has to replace $C_F \to C_A$, and the anomalous dimension. This is influenced by gluon to quark-antiquark splittings. Technically, this can however be taken into account by an extra contribution to the collinear terms, without explicitly generating $g \to q\bar{q}$ splittings.

where $f_i$ are again the fragmentation functions introduced earlier. To improve the logarithmic accuracy, it can be argued that the strong coupling constant should actually be evaluated at a scale of $\mu = k_\mathrm{t}$ [106]. This will be done in the following, i.e. $\alpha_s$ should be read as $\alpha_s(k_\mathrm{T}^2)$ with $k_\mathrm{T}$ suitably expressed through the evolution variable $t$ and the light cone momentum fraction $z$.

Formally, two solutions at different scales $t$ and $t'$ can then be related by the integral equation

$$f(x,t') = \Pi(t',t)f(x,t) + \int_{t'}^{t} \frac{dt''}{t''}\Pi(t'',t') \int \frac{dz}{z}\frac{\alpha_s}{2\pi}P(z)f(x/z,t'') \tag{3.2}$$

where $\Pi$ is the so called Sudakov form factor [107]

$$\Pi(t',t) = e^{-R(t,t')} \ , \tag{3.3}$$

with the single emission probability between two scales and its logarithmic derivative

$$R(t',t) = \int_{t'}^{t} \frac{d\bar{t}}{\bar{t}}\, R'(\bar{t}) \qquad \text{where} \qquad R'(t) = \int_{z_{\min}(t)}^{z_{max}(t)} dz\, \frac{\alpha_s}{2\pi}P(z) \ . \tag{3.4}$$

It is made explicit here that there is some freedom to choose the integration bounds, $z_\mathrm{min}$ and $z_\mathrm{max}$ and that they will generally depend on $t$. It will be seen in the later Section 3.2.1 on resummation, that they are only partially determined by NLL requirements. In a conventional shower algorithm, they are further restricted by the physical requirement of momentum conservation, that dictates they should be chosen as to guarantee $z(1-z) > k_\mathrm{T}^2/Q^2$, see Section 3.1.2. Feasibility, for example the requirement not to work with negative weights, will lead to further changes using the ambiguity at NLL level.

Equation (3.2) is written in a form that has a convenient physical interpretation, which is exploited in parton shower Monte Carlos. It can be stated as follows:

- The first term describes the possibility that there are no emissions between the scales $t$ and $t'$, in which case the distribution remains unchanged.
- The second term integrates over possible additional emissions between the two scales, with a last emission at scale $t''$. The dependence of $f$ on $t''$ in this second term recursively takes arbitrary many emissions between scales $t$ and $t''$ into account.

Thus, the Sudakov form factor $\Pi(t',t)$ is interpreted as the no-emission probability between the two scales. A parton shower algorithm implements this by determining the next scale $t'$ starting from a given scale $t$, according to the distribution

$$\mathcal{P}(t',t) = \frac{d\Pi(t',t)}{d\ln t'} \ . \tag{3.5}$$

and iterating this until a cutoff scale $t_c$ is reached. In a typical implementation, $t_c$ is chosen to mark the transition between the perturbative and non-perturbative regime, e.g $\alpha_s(t)/2\pi \approx 1$.

To simplify the computations, in particular in the direct comparison with resummed calculations for specific observables, the shower will be ordered in the variable

$$\xi = k_T^2\,(1-z)^{-\frac{2b}{a+b}}\ . \tag{3.6}$$

This corresponds, up to a power, to the value of $V(k)$ in Equation (2.17). That can be verified by inserting the definition of $\eta$ in terms of $z$ in the parametrisation given in Section 2.5. The values of $a$ and $b$ are then chosen according to the observable that should be resummed in the shower. For the observables studied in this work, the parameters were given in Table 2.1.

In the semi-analytic CAESAR framework, which will be used for the comparison later, resummed calculations are performed in terms of the cumulative cross section for an observable,

$$\Sigma\,(v) := \frac{1}{\sigma}\int^{v} d\bar{v}\,\frac{d\sigma}{d\bar{v}}\ , \tag{3.7}$$

i.e. the normalised differential cross section integrated up to a value $v$ of the observable considered. In the parton shower formalism, this is just

$$\Sigma_{\mathrm{PS}}(v) = \sum_{m=0}^{\infty}\prod_{i=0}^{m}\frac{1}{m!}\int\frac{d\xi_i}{\xi_i}\mathcal{P}(\xi_i,\xi_{i+1})\Theta(v - V(\xi_1,\ldots,\xi_m))\ . \tag{3.8}$$

Here, $m$ counts the numbers of emissions in a particular event, and is summed over all possible numbers including no emission. The integral is then over the possible values of individual scales at which emissions occur. The integrand accordingly that corresponds to the probability for this emission with no intermediate emissions, or zero if the value of the observable calculated from an event with those emissions would be larger than $v$.

Inserting Equation (3.5) and using (3.3), this parton shower result can explicitly be written as

$$\begin{aligned}\Sigma_{\mathrm{PS}}\,(v) &= \sum_{m=0}^{\infty}\left(\prod_{i=1}^{m}\int_{\xi_c}^{\xi_{i-1}}\frac{d\xi_i}{\xi_i}\,R'_{\mathrm{PS}}(\xi_i)\,e^{-R_{\mathrm{PS}}(\xi_{i-1},\xi_i)}\right)e^{-R_{\mathrm{PS}}(\xi_m,\xi_c)}\\ &\qquad\times\Theta\!\left(v-\sum_{j=1}^{m}V(\xi_j)\right)\Bigg|_{\xi_0=Q^2}\\ &= e^{-R_{\mathrm{PS}}(Q^2,\xi_c)}\sum_{m=0}^{\infty}\frac{1}{m!}\left(\prod_{i=1}^{m}\int_{\xi_c}^{Q^2}\frac{d\xi_i}{\xi_i}\,R'_{\mathrm{PS}}(\xi_i)\right)\\ &\qquad\times\Theta\!\left(v-\sum_{j=1}^{m}\xi_j^{(a+b)/2}\right).\end{aligned} \tag{3.9}$$

To arrive at this result, the approximately additive property of the observables considered here has been used, as well as the particular parametrisation of the observable in terms of $\xi$. It should be kept in mind that both are only valid in the soft limit, while Equation (3.8) holds with more generality.

At the single emission level, during the calculation of $R$, care has to be taken to avoid double counting of the contributions arising in the soft limit [108]. The soft limit is present in the splitting kernels by the terms proportional to $1/(1-z)$, which are enhanced in the limit $z \to 1$. In the corresponding limit of matrix elements, and thus physical cross sections, there is however no distinction between soft limits with respect to different particles. Integrating the soft term over the full available phase space for each hard leg would thus lead to double counting of these contributions.

A standard way to deal with this problem, that is also chosen in the CAESAR formalism which is used in the comparison later, is to restrict the phase space to allow only forward emissions, i.e. with $\eta > 0$, from each leg. This leads to the expression

$$\begin{aligned}R_{\mathrm{PS}}(v) = 2\int_{Q^2 v^{\frac{2}{a+b}}}^{Q^2}\frac{d\xi}{\xi}\int_{z_{\min}}^{z_{\max}}dz\,\frac{\alpha_s\big(\xi(1-z)^{\frac{2b}{a+b}}\big)}{2\pi}\,C_F\left[\frac{2}{1-z}-(1+z)\right]\\ \times\Theta\!\left(\ln\frac{(1-z)^{\frac{2a}{a+b}}}{\xi/Q^2}\right)\end{aligned} \tag{3.10}$$

for the probability of an emission at $\xi > Q^2 v^{2/(a+b)}$ in the parton shower. It is in principle not necessary to restrict the integral of the collinear term. However, this would lead to a negative splitting kernel in the region where only the collinear part would contribute.

Hence this violates the probability conserving interpretation of a unitary parton shower.

It is well known how to deal with this situation in principle [109, 110, 111], and the method to do so will be reviewed for this particular situation in Section 4.1. From the point of view of numerical efficiency, it is however often favourable to avoid the corresponding negative weights. Most traditional parton showers do not have this option implemented. For this reason, the default DGLAP based shower used here will apply the restriction for the soft and collinear term, as shown in Equation (3.10). From a formal point of view this corresponds to a correction that is suppressed by a power of $v$ and therefore is not relevant for logarithmic resummation.

### 3.1.2 Full shower

Conventional parton showers, as used in full fledged Monte Carlo simulations, include more effects than discussed in the previous section even for the simple born process of $e^+e^- \to q\bar{q}$ considered here [13]. Further, modern parton showers often rely on a different treatment of the soft double counting problem described above, which is to factor the soft eikonal. Both will be described here briefly for completeness and as they are used in the analysis in Section 5.2.

#### Full DGLAP Showers

Away from the strict soft limit, emissions will cause a recoil on the hard legs present at born level. Monte Carlo simulations take this into account by generating the four momenta after an emission according to a particular prescription, in the following called recoil scheme. The prescription used later is the one given in [112]. This is, for a parton $ij$ with momentum $\tilde{p}_{ij}$ splitting into partons $i$ and $j$ with respective momenta $p_i$ and $p_j$, with a spectator absorbing the recoil $k$ and changing its momentum from $\tilde{p}_k$ to $p_k$, the new momenta are assigned as follows:

$$p_i = z\tilde{p}_{ij} + (1-z)y\tilde{p}_k + k_\perp \ , \tag{3.11}$$

$$p_j = (1-z)\tilde{p}_{ij} + zy\tilde{p}_k - k_\perp \ , \tag{3.12}$$

$$p_k = (1-y)\tilde{p}_k \ . \tag{3.13}$$

Here $k_\perp$ is a four momentum with $k_\perp^2 = k_\mathrm{T}^2$, the transverse momentum that that is given in the parton shower in terms of the evolution variable and $z$.

The requirement that all momenta are on-shell, $p_i^2 = 0 = p_j^2$, leads to a relation between $z$, $y$ and $k_\mathrm{T}^2$:

$$k_\mathrm{T}^2 = z(1-z)yQ^2 \tag{3.14}$$

with $Q^2$ the invariant mass of the emitting $q\bar{q}$ dipole formed from emitter and spectator, $Q^2 = 2\tilde{p}_{ij} \cdot \tilde{p}_k$.

In the parton shower, $k_{\mathrm{T}}^2$ and therefore $y$ can directly be calculated from the evolution variable and $z$. It should however be noted, that there can be choices of evolution variables that are equivalent in the strict soft-collinear limit but differ away from it, leading to different definitions of the $y$ and $z$ variables above in terms of the shower variables. There are however different ways how to define the evolution variable away from the soft-collinear limit. This leads for example to the different definitions of $k_{\mathrm{T}}$ in the transverse momentum ordered showers compared in Section 5.1.3.

In order to ensure momentum conservation in the $\tilde{p}_k$ direction, it must be required that $0 < y < 1$. As can be seen from Equation (3.13), some particles of the final state would develop negative energies during the emission process. Thus, for momentum conservation to be satisfied, it must thus be required that

$$z(1-z) > k_{\mathrm{T}}^2/Q^2 \tag{3.15}$$

with $Q^2 = 2\tilde{p}_{ij} \cdot \tilde{p}_k$. The parton shower then generates further emissions from the full state including the newly generated particle.

This also implies that they will necessarily include more than one kind of splittings, in particular of the form $g \to gg$ and $g \to q\bar{q}$. The corresponding splitting kernels $P_{gg}$ and $P_{gq}$ are give in Equations (2.12) and (2.13). The exponent encountered in the Sudakov factor contains a sum over the available splittings in this case and will accordingly change after each emission to account for the changed overall state.

### Modern dipole showers

As an alternative treatment of soft double counting is to replace the soft term in the splitting functions by a partial fraction of the soft eikonal matched to the collinear limit [112]. The modification leads to modified splitting kernels,

$$P_{q\bar{q}} = C_F \left[ \frac{2}{1-z(1-y)} - (1+z) \right] \tag{3.16}$$

$$P_{gg} = 2C_A \left[ \frac{1}{1-z(1-y)} + \frac{1}{1-(1-z)(1-y)} - 2 + z(1-z) \right] \tag{3.17}$$

$$P_{gq} = T_R \left[ z^2 + (1-z)^2 \right] \; . \tag{3.18}$$

The equations given here hold for pure final state evolution, i.e. with no coloured particles in the initial state, with massless particles. This effectively regularises the divergences encountered at $z \to 1$. In that way, the $z$-integral can be performed over the whole range $0 < z < 1$. At least in principle, as the constraint $0 < y < 1$ leads to the relation between $z$ and $k_{\mathrm{T}}$ in Equation (3.15), which limits the available $z$ range. It should also be noted that the splitting functions explicitly depend on $y$, which is defined in terms of the four-momentum of the particle absorbing the recoil. This spectator is manifestly part of the formalism, where emissions are pictured as coming from the dipole formed from emitter and spectator rather than from individual partons.

## 3.2 Resummation in the CAESAR formalism

The CAESAR formalism [33] is a particular framework to carry out NLL resummed calculations for specific observables in a semi automated fashion. Suitable observables have to fulfil the properties discussed in Section 2.5. In particular they

- are infrared safe, to ensure that they are well defined in the context of perturbation theory. Further, they have to be recursive infrared safe for the CAESAR formalism to be applicable.
- approach zero smoothly in the $n$-jet limit, where here always the $n = 2$ case is assumed. The observable is then called an $(n + 1)$-jet observable.
- are global, i.e. they have the same scaling behaviour everywhere in phase space as they approach zero.
- can be parametrised when approaching zero as Equation (2.17). If more complicated observables, in particular with $n > 2$ are considered, the formalism might in principle still apply, then with a more general form of Equation (2.17).

The result obtained for $\Sigma(v)$ in this framework is analogous to Equation (3.9) derived in the shower formalism. Parton showers achieve NLL accuracy in the here used examples with trivial color structure. Thus, the only problem remaining is to eliminate subleading contributions, to obtain a leading logarithmic result plus a single logarithmic term.

To formalise the order at which the calculation is performed, it is anticipated that the result will be of the form

$$\ln \Sigma(v) = L g_1(\alpha_s L) + g_2(\alpha_s L), \qquad \text{where} \qquad L = -\ln v \tag{3.19}$$

where $g_1$ and $g_2$ are both power series in $\alpha_s L$ of the form $\sum_n \alpha_s^n L^n$. The terms in $g_1$, which are further enhanced by the additional factor of $L$ in the limit $v \to 0$, are then referred to as leading logarithmic (LL) terms, while the ones in $g_2$ are the single logarithmic terms which enter at the level of NLL computations.[2]

It is convenient here to write results as functions of $L = -\ln v$ rather than $v$, as is done in equation (3.19), as one is interested in the resummation of terms $\propto \ln v$ in

[2] A different counting would be obtained by expanding the exponential in Equation (3.19) and then count the powers of $L$ in this series. This is an alternative definition of logarithmic accuracy, that is not used here but elsewhere in the literature and should be distinguished from the counting that is adopted in accordance with the CAESAR formalism.

the limit $v \to 0$. A contribution that would be $\propto v = e^{-L}$ will vanish in the limit of interest, and can formally always be ignored as far as the analytic resummation of collinear logarithms is concerned.

It should be noted that Equation (3.9) was derived in the simplified version of the shower, in particular in a shower where only emissions from the hard legs present at born level are taken into account. This is correct for recursive infrared observables, as emissions from soft gluons can only contribute inclusive. This can be formally absorbed into the running coupling by redefining it in the Catani-Marchesini-Webber (CMW) scheme [77],

$$\alpha_{\mathrm{CMW}}(k_{\mathrm{T}}^2) = \alpha_{\overline{\mathrm{MS}}}(k_{\mathrm{T}}^2) + \alpha_{\overline{\mathrm{MS}}}^2(k_{\mathrm{T}}^2)K \ . \tag{3.20}$$

In principle there are additional terms proportional to $\ln k_{\mathrm{T}}/\mu$, with $\mu$ being the energy scale at which the strong coupling is calculated. These are absent here as the formula is shown explicit with the choice of $\mu = k_{\mathrm{T}}$ used in the resummation and in the shower. The precise form of the coefficient $K$ also depends on the renormalization scheme, in the $\overline{\mathrm{MS}}$ scheme used here it is given by

$$K = \left(\frac{67}{18} - \frac{\pi^2}{6}\right) C_A - \frac{10}{9} T_R n_f \tag{3.21}$$

with $C_A$, $n_f$ and $T_R$ as defined in Section 2.2.

To eliminate terms in Equation (3.9) that are even further suppressed than the single logarithmic contributions, one might first consider the exponential $e^{-R(\xi_c)}$, where here and in the following, the first argument of $R$ will always be $Q^2$ and hence be suppressed to ease notation. It is then possible to expand $R$ around $v$, recalling that all relevant dependencies are logarithmic,

$$\begin{aligned} R(\xi_c) \approx R_{\mathrm{NLL}}(v) &:= R(v) + R'(v)(\ln v - (a+b)\ln\sqrt{\xi_c/Q^2}) \\ &= R(v) - R'(v)\ln\varepsilon, \qquad \varepsilon = \left(\xi_c/Q^2\right)^{(a+b)/2}/v \end{aligned} \tag{3.22}$$

The dimensionless argument of $R$ should here be understood as being in units of $Q^2$ and meaning the lowest value of the observable allowed, see also Equation (3.24) and the following. Equation 3.9 is than at NLL level of the form

$$\Sigma_{\mathrm{NLL}} = e^{-R(v)}\mathcal{F}(v) \ , \tag{3.23}$$

where $\mathcal{F}$ is just the remaining exponential times the sum over multiple splittings, in the limit $\varepsilon \to 0$:

$$\begin{aligned} \mathcal{F}_\varepsilon(v) &= e^{R'(v)\ln\varepsilon} \sum_{m=0}^{\infty} \frac{1}{m!} \left( \prod_{i=0}^{m} \int_\varepsilon \frac{dv_i}{v_i} R'(v_i) \right) \Theta\left( v - \sum_{j=1}^{m} v_j \right) \ , \\ \mathcal{F}(v) &= \lim_{\varepsilon \to 0} \mathcal{F}_\varepsilon(v) \end{aligned} \tag{3.24}$$

The Jacobian of the necessary transformation has in this case be absorbed into the corresponding change of the derivative of $R$ as $R'(v_i) = \partial R/\partial \ln v_i$. The particular form of $\Sigma$ is key to the CAESAR formalism. The next sections will discuss the analytic computation of $R_{\mathrm{NLL}}$ and the treatment of $\mathcal{F}$, with the elimination of subleading contributions as well as the analytic and numeric computation.

### 3.2.1 Single emission level

The only factor relevant to the cumulative cross section $\Sigma$ at the level of single emissions is the precise form of $R_{\mathrm{NLL}}$, as the only contribution comes from the no-emission probability at a scale larger than $v$:

$$\Sigma_{\substack{\text{single}\\ \text{emission}}}(v) = e^{-R_{\mathrm{NLL}}(v)} \ . \tag{3.25}$$

This already contains all LL terms and additional NLL terms. The single emission integral, in the notation adopted earlier, looks as follows:

$$\begin{aligned} R(v) = \ & 2\int_{Q^2 v^{\frac{2}{a+b}}}^{Q^2} \frac{d\xi}{\xi} \int_0^1 dz \, \frac{\alpha_s\big(\xi(1-z)^{\frac{2b}{a+b}}\big)}{2\pi} \, C_F \left[\frac{2}{1-z}\right] \\ & \qquad\qquad \times \Theta\left(\ln \frac{(1-z)^{\frac{2a}{a+b}}}{\xi/Q^2}\right) \\ & - 2\int_{Q^2 v^{\frac{2}{a+b}}}^{Q^2} \frac{dk_{\mathrm{T}}^2}{k_{\mathrm{T}}^2} \frac{\alpha_s(k_{\mathrm{T}}^2)}{2\pi} \int_0^1 dz(1+z) \ . \end{aligned} \tag{3.26}$$

The Theta function is again used to remove soft double counting, by the method of phase space sectioning as described previously. It has been made explicit that it is actually only necessary for the soft term $\propto 1/(1-z)$.

The collinear term $\propto (1+z)$ is more conveniently analysed by changing the integration variable back from $\xi$ to $k_{\mathrm{T}}^2$, as the allied range is limited as shown in Equation (3.26) to large values of the transverse momentum $k_{\mathrm{T}}^2$. Continuing the integral to lower values of $k_{\mathrm{T}}^2$ would introduce additional terms of higher logarithmic accuracy that are eliminated in the CAESAR formalism.

The precise $z$-integration limits of the collinear term can be modified in logarithmic resummation, as adding a power of $k_{\mathrm{T}}/Q$ for example will only result in a power correction to $\Sigma(v)$ of the form $e^{c_n v^n}$ with some power $n$. It can be ignored at any logarithmic accuracy since it vanishes in the limit of small $v$. Thus, the integration might be carried out over the full range here, leading to the quark anomalous dimension

$$2B_l = -\int_0^1 dz(1+z) = -\frac{3}{2} \ . \tag{3.27}$$

The two loop running terms $\alpha_s^{2L}$, see Equation (2.6), as well as the terms $\propto K$ in the CMW scheme are quadratic in $\alpha_s$. They therefore correspond to NLL corrections when multiplied to the double logarithmic soft terms, and would introduce even higher order terms when being multiplied to the collinear term, which is single logarithmic by itself. They are hence not included in the analytic result for the collinear term.

The single emission integral can now be written as a term capturing the double logarithmic and some of the single logarithmic contributions, plus the anomalous dimension times a single logarithmic term,[3]

$$R_{\mathrm{NLL}}(v) = 2C_F\left(r\left(L\right) + B_l T\left(L\right)\right) \ . \tag{3.28}$$

Here $T(L)$ is the remaining integral over $\alpha_s$, which is only needed at one loop accuracy as discussed above

$$T(L) = \int_{Q^2v^2}^{Q^2} \frac{dk_{\mathrm{T}}^2}{k_{\mathrm{T}}^2}\frac{\alpha_s(k_{\mathrm{T}}^2)}{\pi} = -\frac{1}{\pi\beta_0}\ln(1-2\lambda) \ , \tag{3.29}$$

with $\lambda = \beta_0\alpha_s L$ being a convenient parameter to introduce, as almost all relevant dependencies on $L$ are of this form. The function $r(L)$ can be split into a double and a single logarithmic term,

$$r(L) = Lr_1(L) + r_2(L) \tag{3.30}$$

where $r_1$ is the LL part,[4] again expressed through $\lambda$ defined above,

$$\begin{aligned} r_1(L) = \frac{1}{L}\int_{Q^2v^{\frac{2}{a+b}}}^{Q^2}\frac{d\xi}{\xi}\int_0^1 dz\,\frac{\alpha_s^{1L}\left(\xi(1-z)^{\frac{2b}{a+b}}\right)}{2\pi}\,C_F\left[\frac{2}{1-z}\right] \\ \times\,\Theta\!\left(\ln\frac{(1-z)^{\frac{2a}{a+b}}}{\xi/Q^2}\right) \\ = \frac{1}{2\pi\beta_0\lambda b}\left[(a-2\lambda)\ln\left(1-\frac{2\lambda}{a}\right)\right. \\ \left. -(a+b-2\lambda)\ln\left(1-\frac{2\lambda}{a+b}\right)\right] \ . \end{aligned} \tag{3.31}$$

The functional form of the LL contribution is made explicit by writing it as a power series $r_1$ in $\alpha_s L$ which is multiplied by another factor of $L$ as in Equation (3.30).

[3] The notation here mimics that of reference [33]. The equations are however adapted to the simplified setup of two jet observables with $d = g(\Phi) = 1$ in the center of mass frame with $Q$ chosen to be the center of mass energy. They would have to be generalised to capture the full case.

[4] To carry out the actual integration, it is more convenient to change the integration variable back to $k_{\mathrm{T}}^2$ and perform the analysis of reference [33].

The NLL piece $r_2$ is calculated from the same integral but corresponds to the terms including $\alpha_s^2$ terms,

$$\begin{aligned}
r_2(L) = &\int_{Q^2 v^{\frac{2}{a+b}}}^{Q^2} \frac{d\xi}{\xi} \int_0^1 dz\, \frac{\alpha_s^{2L}\big(\xi(1-z)^{\frac{2b}{a+b}}\big)}{2\pi} C_F \left[\frac{2}{1-z}\right] \\
&\qquad\qquad \times \Theta\!\left(\ln \frac{(1-z)^{\frac{2a}{a+b}}}{\xi/Q^2}\right) \\
&+ \int_{Q^2 v^{\frac{2}{a+b}}}^{Q^2} \frac{d\xi}{\xi} \int_0^1 dz\, K \left(\frac{\alpha_s^{1L}\big(\xi(1-z)^{\frac{2b}{a+b}}\big)}{2\pi}\right)^2 C_F \left[\frac{2}{1-z}\right] \\
&\qquad\qquad \times \Theta\!\left(\ln \frac{(1-z)^{\frac{2a}{a+b}}}{\xi/Q^2}\right) \\
= &\frac{1}{b}\left[\frac{\beta_1}{2\pi\beta_0^3}\left(\frac{a}{2}\ln^2\left(1-\frac{2\lambda}{a}\right) - \frac{a+b}{2}\ln^2\left(1-\frac{2\lambda}{a+b}\right)\right.\right. \\
&\qquad \left. + a\ln\left(1-\frac{2\lambda}{a}\right) - (a+b)\ln\left(1-\frac{2\lambda}{a+b}\right)\right) \\
&\left. \frac{K}{(2\pi\beta_0)^2}\left((a+b)\ln\left(1-\frac{2\lambda}{a+b}\right) - a\ln\left(1-\frac{2\lambda}{a}\right)\right)\right].
\end{aligned} \tag{3.32}$$

For the case of $b = 0$, like the fractional energy correlation with $x = 1$ discussed here, the corresponding limit has to be taken. It can be verified that it always exists and is finite.

The Landau pole in the evolution of the strong coupling is visible in the expressions for $r_1$ and $r_2$ as the logarithmic branch cut. For example for an observable that scales like (a power of) the transverse momentum, $v \sim k_\mathrm{T}$, in the soft-collinear limit, the first one would be at $\lambda = \beta_0\alpha_s \ln k_\mathrm{t}/Q = 1/2$ corresponding to the pole at $k_\mathrm{T} = Qe^{-1/2\alpha_s\beta_0}$ found in Section 2.2.

The above discussion also shows that the logarithmic derivative of $R$ will be at most single logarithmic. As $T$ and $r_2$ are already single logarithmic themselves, all that is left is

$$R'(v) = 2C_F r'(L), \quad r'(L) = \partial_L L r_1(L) \tag{3.33}$$

This can conveniently be expressed through $T$ as

$$
\begin{aligned}
r'(L) &= \frac{1}{b}\left[T\left(\frac{L}{a}\right) - T\left(\frac{L}{a+b}\right)\right] \\
&\to \frac{2}{a^2}\frac{1}{\pi\beta_0}\frac{\lambda}{1-2\lambda/a} \qquad \text{as} \qquad b \to 0
\end{aligned}
\tag{3.34}
$$

### 3.2.2 Multiple emissions

As argued in reference [33], for the purpose of calculating the $\mathcal{F}$-function, the difference between $\alpha_s \ln v_i$ and $\alpha_s \ln v$ is subleading. Hence, in equation (3.24) one might replace $R'(v_i) \to R'(v)$ under the integral,

$$
\mathcal{F}_\varepsilon^{\mathrm{NLL}}(v) = e^{R'(v)\ln\varepsilon} \sum_{m=0}^{\infty} \frac{R'^m(v)}{m!} \prod_{i=0}^{m} \int_\varepsilon^1 \frac{d\zeta_i}{\zeta_i} \Theta(1 - \sum_j \zeta_j), \tag{3.35}
$$

where the dimensionless integration variables $\zeta_i v_i/v$ have been introduced. Writing the Theta-function explicit as an integral representation,

$$
\begin{aligned}
\mathcal{F}_\varepsilon^{\mathrm{NLL}}(v) &= \int \frac{d\nu}{2\pi i\nu} e^{\nu} e^{R'(v)\ln\varepsilon} \sum_{m=0}^{\infty} \frac{R'^m(v)}{m!} \prod_{i=0}^{m} \int_\varepsilon^1 \frac{d\zeta_i}{\zeta_i} e^{-\nu\zeta_i} \\
&= \int \frac{d\nu}{2\pi i\nu} e^{\nu + R'(v)\int_\varepsilon^1 \frac{d\zeta_i}{\zeta_i}(e^{-\nu\zeta_i}-1)}
\end{aligned}
\tag{3.36}
$$

At NLL accuracy, one might further replace the exponential factor by a phase-space boundary $(e^{-\nu\zeta_i} - 1) \to -\Theta\left(\zeta_i - e^{-\gamma_E}/\nu\right)$ under the integral in the exponent [20, 113, 114]. Here $\gamma_E$ is the Euler-Mascheroni constant. The remaining integral can be solved to give

$$
\mathcal{F}^{\mathrm{NLL}}(v) = \frac{e^{-\gamma_E R'(v)}}{\Gamma\left[1 + R'(v)\right]} \,. \tag{3.37}
$$

This result holds for all additive observables that can be resummed in the CAESAR formalism, even if more coloured legs are present at born level, with suitable adjustments to $R'$ like summing over the additional legs with in general different contributions. At NLL accuracy, the unphysical dependence on $\varepsilon$ has cancelled. If the integral is not performed analytically as shown above but numerically starting from Equation (3.35), a residual dependence on $\varepsilon$ will remain.

Fortunately, the series converges rather fast for moderate $\varepsilon \gtrsim 0.1$, such that this dependence can be determined from the first few terms in order to confirm the correct behaviour of the numerical result as $\varepsilon$ approaches zero. The convergence is shown in Figure 3.1 at the example of the thrust observable $1 - T$, cf Equation (2.18). For

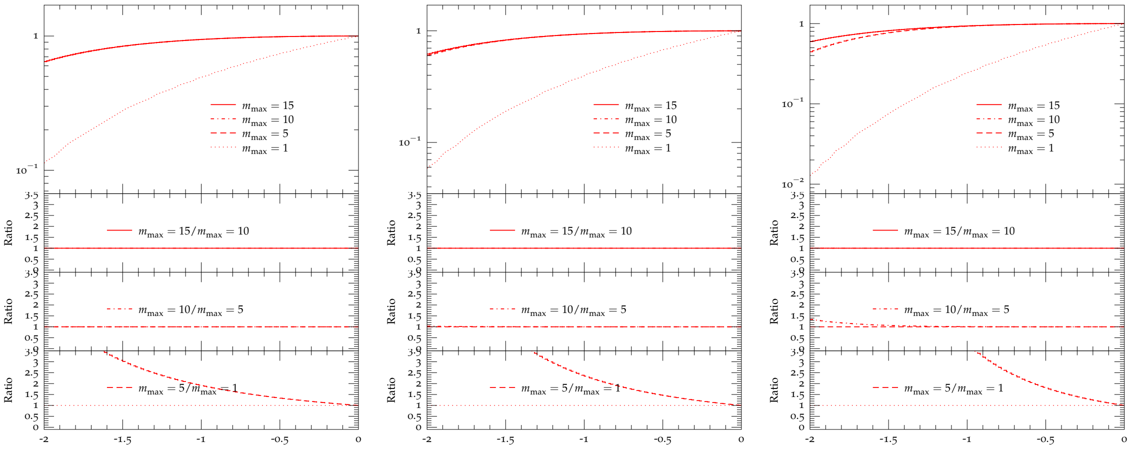


(a) $\varepsilon = 0.1$ (b) $\varepsilon = 0.05$ (c) $\varepsilon = 0.01$

Figure 3.1: Convergence of the $\mathcal{F}$ function for the thrust observable $1 - T$, calculated from the first $m_{\max}$ terms of the sum in Equation (3.35), for different values of $\varepsilon$. Shown are the cases $\varepsilon = 0.1$ (a), $\varepsilon = 0.05$ (b) and $\varepsilon = 0.01$ (c) calculated from the first and the first 5, 10 and 15 terms. For the $\varepsilon = 0.1$ case, only the first 10 terms can contribute.

relatively large $\varepsilon = 0.1$, of course only the first 10 terms can contribute in principle. It can however be seen that the series converges much faster, and already the 5th term is numerically not very relevant.

Only for $\varepsilon = 0.01$, a significant dependence change is observed from including the 10th term, although also this is at the level of few percent. In Section 4.3, it will be seen that for $\varepsilon \approx 0.001$, the shower can be compared to the analytic result oft $\varepsilon \to 0$ in Equation (3.37). In this case, terms with many emissions, up to $\sim 20$, become increasingly relevant. In this case, it becomes to cumbersome to calculate the residual dependence on $\varepsilon$ explicitly in a reliable way from summing the first few terms. The results will thus be directly compared to the full result.

## 3.3 Parton shower and CAESAR formalism in a common language

After developing the parton shower formalism and resummation in the CAESAR framework in the previous sections, this section describes repreats the main results in a common language. the adaptions necessary in the parton shower to resemble the pure NLL result are highlighted. This establishes the notation necessary to name the differences analysed in Chapter 5.

It is possible to write the parton shower and the analytic result in a similar notation as

$$\Sigma(v) = \exp\left\{-\int_v \frac{d\xi}{\xi} R'_{>v}(\xi) - \int_{v_{\min}}^{v} \frac{d\xi}{\xi} R'_{<v}(\xi)\right\} \times \sum_{m=0}^{\infty} \frac{1}{m!} \left(\prod_{i=1}^{m} \int_{v_{\min}} \frac{d\xi_i}{\xi_i} R'_{<v}(\xi_i)\right) \Theta\left(v - \sum_{j=1}^{m} V(\xi_j)\right) . \tag{3.38}$$

with $R'_{<v}$ and $R'_{>v}$ given by the following:

$$\begin{aligned} R'_{\lessgtr v}(\xi) = & \frac{\alpha_s^{\lessgtr v,\mathrm{soft}}\left(\mu^2_{\lessgtr}\right)}{\pi} \int_{z^{\min}}^{z^{\max}_{\lessgtr v,\mathrm{soft}}} dz\, C_F \frac{1}{1-z} \\ & - \frac{\alpha_s^{\lessgtr v,\mathrm{coll}}\left(\mu^2_{\lessgtr v}\right)}{\pi} \int_{z^{\min}}^{z^{\max}_{\lessgtr v,\mathrm{coll}}} dz\, C_{\mathrm{F}} \frac{1+z}{2} . \end{aligned} \tag{3.39}$$

The parameters to reproduce the analytic and the parton shower result respectively are given in Table 3.1 and will be explained below.

At one emission level, the only difference is in the exact computation of the single emission integral $R$. The parton shower result was given in Equation (3.10) as

$$\begin{aligned} R_{\mathrm{PS}}(v) = 2 \int_{Q^2 v^{\frac{2}{a+b}}}^{Q^2} \frac{d\xi}{\xi} \int_{z_{\min}}^{z_{\max}} dz\, \frac{\alpha_s\left(\xi(1-z)^{\frac{2b}{a+b}}\right)}{2\pi} C_F \left[\frac{2}{1-z} - (1+z)\right] \\ \times \Theta\left(\ln \frac{(1-z)^{\frac{2a}{a+b}}}{\xi/Q^2}\right) , \end{aligned}$$

The values if the $z$ integration bounds are given by the kinematic constraint from Equation (3.14) discussed earlier.

The analytic result was shown in Section 3.2, Equation (3.22) and read:

$$\begin{aligned} R_{\mathrm{NLL}}(v) = 2 \int_{Q^2 v^{\frac{2}{a+b}}}^{Q^2} \frac{d\xi}{\xi} \Bigg[ \int_0^1 dz\, \frac{\alpha_s\left(\xi(1-z)^{\frac{2b}{a+b}}\right)}{2\pi} \frac{2\,C_F}{1-z} \Theta\left(\ln \frac{(1-z)^{\frac{2a}{a+b}}}{\xi/Q^2}\right) \\ - \frac{\alpha_s(\xi)}{\pi} C_F B_q \Bigg] . \end{aligned}$$

Comparing the two equations, it is necessary to make the following modifications in a parton shower in order to reproduce the pure NLL result:

- The $z$-integration in the soft term runs from 0 to $1 - (\xi/Q^2)^{(a+b)/2a}$, where the upper bound stems from the requirement that $\eta > 0$ (the $\Theta$-function in Equation (3.10)), eliminating the double counting of soft-gluon radiation, but ignoring the other phase space constraints.

| | Resummation | Parton Shower | Figure |
|---|---|---|---|
| $z^{\max}_{>v,\mathrm{soft}}$ | $1-(\xi/Q^2)^{\frac{a+b}{2a}}$ | | n.a. |
| $\mu^2_{>v,\mathrm{soft}}$ | $\xi(1-z)^{\frac{2b}{a+b}}$ | | n.a. |
| $\alpha_s^{>v,\mathrm{soft}}$ | 2-loop CMW | | n.a. |
| $z^{\max}_{>v,\mathrm{coll}}$ | 1 | $1-(\xi/Q^2)^{\frac{a+b}{2a}}$ | 5.1 |
| $\mu^2_{>v,\mathrm{coll}}$ | $\xi$ | $\xi(1-z)^{\frac{2b}{a+b}}$ | 5.1 |
| $\alpha_s^{>v,\mathrm{coll}}$ | 1-loop | 2-loop CMW | 5.4 |
| $z^{\max}_{<v,\mathrm{soft}}$ | $1-v^{\frac{1}{a}}$ | $1-(\xi/Q^2)^{\frac{a+b}{2a}}$ | 5.2 |
| $\mu^2_{<v,\mathrm{soft}}$ | $Q^2v^{\frac{2}{a+b}}(1-z)^{\frac{2b}{a+b}}$ | $\xi(1-z)^{\frac{2b}{a+b}}$ | 5.2 |
| $\alpha_s^{<v,\mathrm{soft}}$ | 1-loop | 2-loop CMW | 5.4 |
| $z^{\max}_{<v,\mathrm{coll}}$ | 0 | $1-(\xi/Q^2)^{\frac{a+b}{2a}}$ | 5.5 |
| $\mu^2_{<v,\mathrm{coll}}$ | n.a. | $\xi(1-z)^{\frac{2b}{a+b}}$ | 5.5 |
| $\alpha_s^{<v,\mathrm{coll}}$ | n.a. | 2-loop CMW | 5.5 |

Table 3.1: Choices of parameters in Equation (3.38) leading to Equation (3.23) (NLL resummation) and Equation (3.9) (parton shower). The effects of switching between the two parametrizations are investigated in the figure referred to in the last column.

- The collinear term proportional to $(1+z)$ is integrated from 0 to 1 in order to produce the collinear anomalous dimension, $B_q$. At the same time, $\alpha_s$ is evaluated at $\xi$.

This is reflected in the parameters given in Table 3.1 for $R'_{>v}$ in the resummation case.

The parameters given for for $R_{<v}$, where effects of multiple emissions are computed can be verified explicitly to reproduce the $\mathcal{F}$-function of Equation (3.23) as it is computed in the analytic formalism and was given here in Equation (3.35) when inserted into Equation (3.38). In particular, the terms of higher logarithmic accuracy in $R'$ have to be dropped, and $R'$ should be calculated at $v$. This can be satisfied by the following modifications to the parton shower:

- The $z$-integration in the soft term runs from 0 to $1-v^{1/a}$. This restricts the phase space that is available to further emissions, at least in the region of large $z$. At small $z$ however, the restriction from momentum conservation is removed from the shower.

- The strong coupling runs at one loop and is evaluated at $v^{2/(a+b)}(1-z)^{2b/(a+b)}$. This is a subleading effect, as a change of the scales, or a higher loop contribution as well as terms associated with the CMW prescription would correspond to an effect of order $\alpha_s$. As the $R'(v)$ function calculated in this range is only single logarithmic, this corresponds to a NNLL ambiguity.

- The collinear term is dropped. As for the previous point, already the contributions coming from soft enhanced part of the splitting function are single logarithmic. One can thus drop the collinear term at NLL accuracy.

# 4 Implementation of resummation as a Markov chain Monte Carlo

In this section, details of the implementation used for the comparison will be given. First, the numerical method of the Sudakov algorithm, adapted to the notation used here, will be reviewed including modifications of the original version [115], which have been introduced in the literature to handle negative weights and efficiency issues for particular problems and which are necessary for the study presented here. In the section following that, the details of the implementation necessary to resemble pure NLL results will be given. It will be verified numerically that this is achieved. The logarithmic accuracy of the shower implementations will be validated.

## 4.1 The Sudakov veto algorithm

Parton shower Monte Carlos are implementations of the Sudakov veto algorithm. The general problem is to generate emissions with a no-emission probability,[1] $\Delta(t,t') = e^{F_t(t')}$. The second argument of $\Delta$ has been moved to a subscript of $F$, as it is not necessary for the formalism here where it just labels the state from which the algorithm starts. In the case of interest here $F$ is given by the integral

$$F_t(t') = -\int_{t'}^{t} d\bar{t} \int_{z_{\min}(\bar{t})}^{z_{\max}(\bar{t})} dz\, f(\bar{t},z)\ . \tag{4.1}$$

The algorithm described in this section does not depend on the form of the function to be exponentiated, which is made explicit by using generic symbols. The integration over the $z$ variable is shown explicitly, to highlight that it can be computed numerically within the same formalism, such that no explicit computation of it is necessary in the algorithm. Of course, the following would also apply to functions of just one variable with corresponding modifications, or if it is more convenient to analytically perform the integral, for example if there is no interest in distributions that differential resolve $z$ and the integral is sufficient simple.

Formally, to determine the next value $t'$ after $t$, one just needs to solve the equation

$$\mathcal{R} = \frac{\Delta(t,t_c)}{\Delta(t',t_c)} = e^{F_t(t')} \tag{4.2}$$

with a uniform distributed (pseudo-)random number $\mathcal{R} \in [0,1)$. Assuming $F_t$ and in particular its inverse $F_t^{-1}(t')$ are known analytically, one can immediately solve for the new point $t'$,

$$t' = F_t^{-1}(t + \ln \mathcal{R})\ . \tag{4.3}$$

[1] While the probabilistic interpretation of the algorithm is convenient as long as $f(t,z)$ is strictly positive definite, it is not mandatory and one might picture the algorithm described here as an efficient way to choose the $\xi_i$'s needed to numerically compute (a sum of) integrals of the form in Equation (3.8) with the correct weights. In that sense, a parton shower is a particular implementation of a Markov chain Monte Carlo technique.

In simple cases, like the nuclear decay of an ensemble of radioactive nuclei, in which case $\int dz\, f(t,z) = \text{const.}$, these conditions are met and the above steps can be used to generate for example Poisson distributed values. However often this is not possible, in particular when the inverse function $F^{-1}$ is not known or at least too cumbersome to compute.

It is then often still possible to find an overestimate $g(t,z) > f(t,z)$ and if necessary overestimates $z'_{\text{min}} < z_{\text{min}}(t)$, $z'_{\text{max}} > z_{\text{max}}(t)$, such that

$$G_t(t') = -\int_{t'}^{t} d\bar{t} \int_{z'_{\text{min}}}^{z'_{\text{max}}} dz\, g(\bar{t}, z) \ . \tag{4.4}$$

and the inverse function $G_t^{-1}(t')$ can be computed easily. The new integration limits $z'_{\text{min}}$ and $z'_{\text{max}}$ are here commonly referred to as overestimates, meaning that they are chosen as to overestimate the $z$ integral in Equation (4.1). New values for $t'$ can now be proposed according to Equation (4.4), i.e. $t' = G_t^{-1}(t + \ln \mathcal{R})$. At the same time, the $z$ integral can be performed numerically by generating a proposed value for $z$ according to $\int_{z'_{\text{min}}}^{z'_{\text{max}}} dz\, g(t', z)$, to arrive at a proposed variable pair $(t', z)$ for the emission. This amounts to solving the equation

$$\mathcal{R}' \int_{z'_{\text{min}}}^{z'_{\text{max}}} dz\, g(t', z) = \int_{z'_{\text{min}}}^{z} dz\, g(t', z) \tag{4.5}$$

for z, either analytical or numerical. The random number is called $\mathcal{R}'$ here to distinguish it from the $\mathcal{R}$ that was used to generate $t'$, although both are taken uniformly distributed on the interval $[0, 1)$. The effective weight for an emission so far is given by

$$dz\, dt'\, \mathcal{P}_{\substack{\text{no}\\ \text{veto}}}(t', z) = dz\, dt'\, g(t', z) e^{G_t(t')} \ . \tag{4.6}$$

As long as $0 < f(t,z) < g(t,z)$ holds for all $(t,z)$, that is, the integrand in Equation (4.1) is positive definite, this can simply be corrected to the original distribution aimed for by vetoing events with a probability $1 - f(t',z)/g(t',z)$ and correspondingly accept them with probability $f(t',z)/g(t',z)$. With that, Equation (4.6) will change to

$$\begin{aligned} dz\, dt'\, \mathcal{P}(t', z) = dz\, dt' &\underbrace{\frac{f(t', z)}{g(t', z)}}_{\substack{\text{probability}\\ \text{to accept } t',z}} \underbrace{g(t', z) e^{G_{t_m}(t')}}_{\substack{\text{probability}\\ \text{to propose } t',z}} \\ &\times \frac{1}{m!} \prod_{\substack{z_i, t_i\\ \text{vetoed}}}^{m} \int dt_i\, dz_i \underbrace{\left(1 - \frac{f(t_i, z)}{g(t_i, z)}\right)}_{\substack{\text{probability}\\ \text{to veto } t_i,z_i}} \\ &\qquad\qquad \times \underbrace{g(t_i, z_i) e^{G_{t_{i-1}}(t_i)}}_{\substack{\text{probability}\\ \text{to propose } t_i,z_i}} \ . \end{aligned} \tag{4.7}$$

The product runs over all points $(z_i, t_i)$ that are proposed in the first part of the algorithm but then vetoed, where here $t_0$ denotes the overall starting scale $t_0 = t$, and there are $m$ proposed emissions before the first splitting is accepted. It is assumed that the $t_i$'s in the second line are not ordered, which introduces the combinatorial factor $1/m!$.

The veto effectively amounts to multiply them by a weight that corresponds to the probability for the veto. Note that the label for the starting point of $G_t(t')$ changes with $i$ in the second line of Equation (4.7), such that the different factors of $e^G$ can be combined to give $e^{G_{t_m}(t')} \prod_{i=0}^{m} e^{G_{t_{i-1}}(t_i)} = e^{G_t(t')}$. The remaining integral in the second line will reproduce an additional factor $e^{F_t(t')-G_t(t')}$, which combined with the previous factor of $e^{G_t(t')}$ gives the correct no-emission probability. One arrives at the expected

$$dz\, dt'\, \mathcal{P}(t', z) = dz\, dt'\, f(t', z) e^{F_t(t')} \ . \tag{4.8}$$

While in the above description, the weights $f/g$ and $1-f/g$ corresponding to acceptance and veto are included numerically by actually ignoring the corresponding emissions, they could as well be partially applied analytically by modifying the overall weight of the event. This is useful if $f$ is not of definite sign, i.e. if it turns negative for some values of $t$ and $z$.

The general methods to treat this problem are well known [109, 110, 111]. In the implementation used in this work, a second overestimate $h(t, z)$ is introduced, that is positive for all $t, z$, and can be chosen to be the overestimate that would be used in the standard algorithm. The overestimate $g(t, z)$ is chosen in a way that ensures that $f/g$ is always positive, i.e. $f(t, z)$ and $g(t, z)$ always have the same sign. That way, the veto can still be performed as before, leading to

$$\begin{aligned} dz\, dt'\, \mathcal{P}(t', z) = dz\, dt' \quad & \frac{f(t', z)}{g(t', z)} \quad h(t', z) e^{H_{t_m}(t')} \\ & \times \frac{1}{m!} \prod_{\substack{z_i, t_i \\ \text{vetoed}}}^{m} \int dt_i\, dz_i \left(1 - \frac{f(t_i, z)}{g(t_i, z)}\right) \\ & \qquad \times h(t_i, z_i) e^{H_{t_{i-1}}(t_i)} \ , \end{aligned} \tag{4.9}$$

where $H_t(t')$ denotes the analogous integral over $h$ as before, see Equation (4.1). The remaining weight needed to restore Equation (4.7) is given by

$$\omega = \frac{g(t', z)}{h(t', z)} \prod_{\substack{z_i, t_i \\ \text{vetoed}}} \frac{g(t_i, z_i)}{h(t_i, z_i)} \frac{h(t_i, z_i) - f(t_i, z_i)}{g(t_i, z_i) - f(t_i, z_i)} \tag{4.10}$$

The first term corrects the weight for accepted emissions, the product over the vetoed emissions leads to the exponentiation of the correct factors. The weights in Equation (4.10) can now explicitly become negative.

## 4.2 Details of the implementation

The parton shower described in Section 3.1.1 already achieves NLL accuracy in the simple cases under consideration in this work, it remains however to remove subleading terms in order to exactly resemble a pure NLL resummation by introducing the changes detailed in Section 3.3. As seen there, when using the same method to treat the problem of soft double counting, parton shower and resummation are already very similar at the level of the first emission. The differences lie in the $z$ integration bounds, in particular for the collinear term and in the lower bound for the soft term. These differences also introduce a change in the scale of the running coupling in Equation (3.38). The choice of integration boundaries in the analytic resummation implies that the splitting function turns negative in parts of the phase space. The same happens if the collinear term is not restricted in the same way as the soft term but only by momentum conservation in the shower.

In the specific implementation used here, splittings are generated according to an overestimate of the strong coupling and the splitting kernel

$$\alpha_s^{\max} P_{\max}(z) = \alpha_s^{\max} C_{\mathrm{F}} \left[ \frac{2}{1-z} \Theta\left(z'_{\max} - z\right) + \gamma \Theta\left(z - z'_{\max}\right) \right] \tag{4.11}$$

with an in principle arbitrary constant $\gamma$. For practical calculations a value of $\gamma = 2$ is chosen. Note that the values of $z_{\mathrm{soft}}^{\max}$ and $z_{\mathrm{coll}}^{\max}$ are overestimated by a common value in $P_{\max}$, which is made explicit by writing $z'_{max}$. Splittings are vetoed with a constant probability $1/C$ and are associated with a weight

$$\omega = \frac{C\ \alpha_s^{\mathrm{res}} P_{\mathrm{res}}(z)}{\alpha_s^{\max} P_{\max}(z)} \times \begin{cases} 1 & \text{if accepted} \\ \dfrac{\alpha_s^{max} P_{\max}(z) - \alpha_s^{res} P_{\mathrm{res}}(z)}{(C-1)\,\alpha_s^{res} P_{\mathrm{res}}(z)} & \text{if rejected} \end{cases} \tag{4.12}$$

This correction accounts in particular for the negative sign of the integrand, Equation (4.13), in the region $z > z_{\max}^{\mathrm{soft}}$. In addition, it is possible to veto emissions violating the condition $\sum_i V(k_i) < v$, which would contribute with zero weight, to improve numerical accuracy [110]. The value of $C$ determines how many emissions are proposed, and thus potentially vetoed. It can again in principle be an arbitrary constant larger than 1, but is relevant for the speed of convergence. It is chosen as $C = 2$ in the implementation used here.

The kernel eventually used for NLL resummation needs to respect that there are different integration ranges for the $z$ integration in the different regions. It is given by

$$\alpha_s^{\mathrm{res}} P_{\mathrm{res}} = C_{\mathrm{F}} \left[ \alpha_s(\mu_{\mathrm{soft}}^2) \frac{2}{1-z} \Theta\left(z_{soft}^{\max} - z\right) - \alpha_s(\mu_{coll}^2)(1+z)\Theta\left(z_{coll}^{\max} - z\right) \right] , \tag{4.13}$$

with $z_{\max}$ and $\mu^2$ chosen according to Table 3.1.

For multiple emissions $P_{\text{res}}$ explicitly depends on $v$. Therefore the procedure used here is to first choose a value for $v$ and then run the parton shower, implementing the $z$ integration boundaries and the scale of the strong coupling as defined in Table 3.1. This is a highly inefficient procedure to compute the cumulative cross section.

If probability was conserved, the same distribution could be obtained by running the parton shower, computing $v$, filling the histogram in each bin with lower edge larger than $v$, and filling the histogram in the bin containing $v$ with weight $(v_{max} - v)/\Delta v$, where $v_{max}$ is the upper bin edge and $\Delta v$ is the bin width. This will be the method used to compute the predictions in Figure 5.5 and Sec. **??**.

## 4.3 Validation

The above choices of estimates and weights will finally reproduce the analytic prediction of the CAESAR formalism from the parton shower. This will be verified in this section, by comparing the results of parton shower and resummation and by explicitly evaluating the behaviour of the shower at small values of the observable $v$ where agreement with the resummation is expected in any case.

At the level of accuracy of interest here, it is sufficient to set the cutoff scale of the parton shower to some numerically small value in $\xi$. Exact agreement with the analytic calculation is expected only if the calculation is performed for a finite $\varepsilon$, and the parton-shower cutoff $\xi_x$ is set as defined by $\varepsilon$ in Equation (3.22). One can verify that in this situation the analytic result for finite $\varepsilon$ are reproduced, and investigate the convergence towards the analytic result for $\varepsilon \to 0$. The analytic result is computed here from the first few terms in the sum, as shown in Section 3.2.2. Only for the final case of $\varepsilon = 0.001$, the shower result is compared to the limiting case of $\varepsilon \to 0$.

Figure 4.1 presents the corresponding comparison for different values of $\varepsilon$ in the case of the thrust observable (a), the BKS observable (b) and the fractional energy correlation (c) [33] that were introduced in Section 2.5 where also the related resummation coefficients were given. This shows that the algorithm described in this chapter, in particular with the weights detailed in Section 4.2, is capable of correctly reproducing the pure NLL results of the CAESAR formalism.

To further confirm the logarithmic correctness of the showers used here, in particular that of the full DGLAP shower and the more advanced shower used for the analysis carried out in Section 5.2, one can check that the behaviour of $R'_{\text{PS}}(v)$ is correct in the limit of small $v$. To be able to investigate that limit, $\alpha_s$ will be fixed at $\alpha_s = 0.118$, as otherwise $\alpha_s$ would have to be evaluated at scales way to small for perturbation

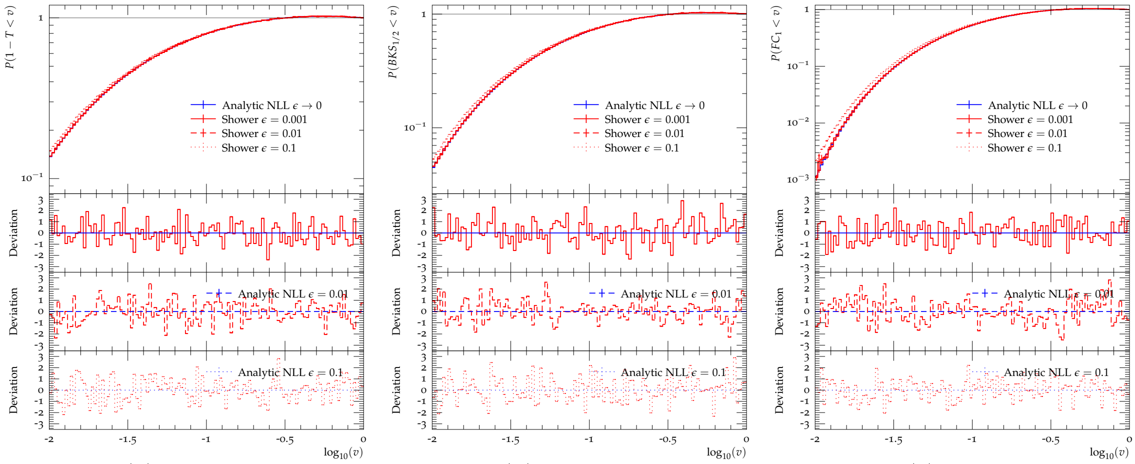


(a) Thrust (b) $\mathrm{BKS}_{1/2}$ (c) $\mathrm{FC}_1$

Figure 4.1: Thrust variable $1-T$ (a), BKS observable with $x = 1/2$ (b) and fractional energy correlation with $x = 1$ (c) for different values of the cutoff $\epsilon$ in Equation (**??**). The respective analytic results for $\mathcal{F}_\epsilon(v)$ are used as a reference in the ratio plots.

theory to be valid in order to observe the convergence to the expected values. This test is performed for a $k_\mathrm{T}$ ordered shower, that is with $v = k_\mathrm{T}^2/Q^2$. Showers for other observables are related to this by a simple integral transformation.

The size of $R_\mathrm{PS}(v)$ can be extracted easily from the shower. The number of emissions between two scales is just Poisson distributed with parameter $R(t, t')$, so $R_\mathrm{PS}(v)$ can be obtained by computing the average number of emissions in the shower when starting from $Q^2$ and developing down to the scale corresponding to $v$. During this procedure, only emissions from the hard quarks present at born level are allowed in all showers, to retrieve comparable quantities.

The average number of emissions per bin, $\langle n \rangle$, then corresponds approximately to the value of $R'_\mathrm{PS}(v)$. In the resummation with fixed $\alpha_s$, one expects a result of the form

$$\frac{\pi}{\alpha_S} R'(v) = C_F \left(L + B_q\right) \ , \tag{4.14}$$

which gives a linear dependence in the logarithmic plot in Figure 4.2. In particular, the slope of the line corresponds to the Casimir factor $C_F$, while the anomalous dimension can be read off from the intersection with zero. The resummation shower exactly reproduces this.

The other showers have further contributions from power suppressed corrections $\propto v$ to $R'$, which as expected vanish in the limit of small $k_\mathrm{T}$, such that a line with slope

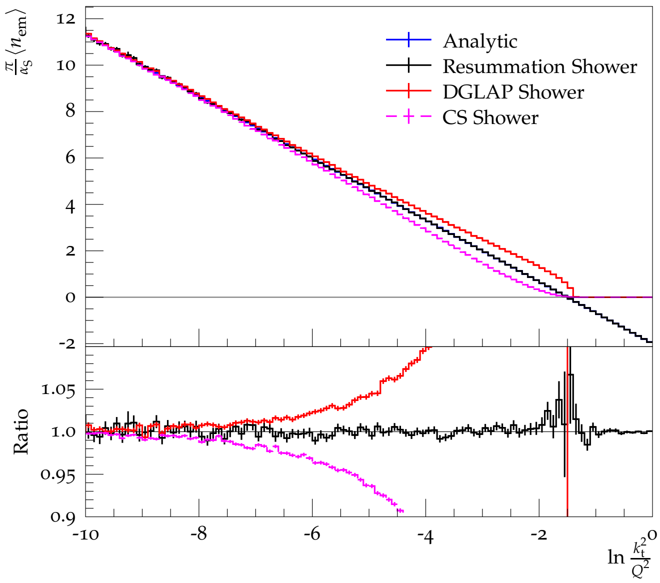


Figure 4.2: Comparison of analytic and parton-shower predictions for the emission probabilities in Equations (3.10) and (3.26). The plot shows the average number of emissions per bin as a proxy observable [110].

$C_F$ is approached also for these cases. This establishes that all showers used in this study correctly reproduce the leading and next to leading logarithmic behaviour, and all differences discussed here are truly subleading.

# 5 Numerical differences between parton shower and analytic resummation

This chapter presents the actual comparison of the parton shower and the analytically resummed calculation. The notation set up in Section 3.3 is used to cast the two formalisms described in chapters 3.1.1 and 3.2 in a common language. Here, the numerical effects on $\Sigma(v)$ of the approximations are investigated in detail. Starting from the resummation shower that mimics the resummation, part of the additional effects that are present in the default DGLAP parton shower are turned on. Finally, the results are compared to the more contemporary dipole parton showers.

While some of the choices in the parton shower are physically motivated, they are clearly subleading, and there is no clear formal preference for any of the choices. In that sense, the changes shown here should be taken as systematic uncertainties that still exist at the NLL level of accuracy, and are in some cases inherent to the resummation of infrared logarithms.

## 5.1 Effects of approximations

This section is dedicated to the detailed investigation of the effects of local four-momentum conservation and approximations made in the NLL calculation compared to the parton shower, which is the main result of this work. In order to cover different choices of the parameters $a$ and $b$ in Equation (2.17), there are again results for the thrust, a BKS observable ($x = 1/2$) and a fractional energy correlation ($x = 1$) presented here as discussed in Section 2.5 where the corresponding parameters were shown in Table 2.1 in Section 2.5.

All distributions are shown for $Q = 91.2$ GeV, and for a strong coupling defined by $\alpha_s(Q^2) = 0.118$ and a fixed number of flavors, $n_f = 5$, as was anticipated in the previous sections. The results have been cross checked between two implementations [1], to further prove their validity. All plots shown here are exactly reproduced by the second, independent code.

### 5.1.1 Single emission level

As seen in Section 3.3, there are already changes between analytic calculation at the level of single emissions. This corresponds to the computation of $e^{-R(v)}$, which can be interpreted as the probability for no emission with an value of the observable larger than $v$. It is then not important at which scale the emission finally happens. As seen in Section 3.2, this already captures the leading logarithmic behaviour.

Differences between shower and analytic resummation in particular stem from different choices to make in the computation of the single emission integrand $R'_{>v}(v)$. First, there is the constraint from momentum conservation in the anti-collinear direction, from Equation (3.14), that constrains

$$Q^2 > 2p_ip_j = \frac{k_T^2}{z(1-z)} \,.$$

This induces both a lower and an upper bound on $z$ given by $z_{\text{min/max}} = (1 \mp \sqrt{1-4k_T^2/Q^2})/2$. This constraint is not easily expressed through $\xi$, and thus formulated and implemented directly in terms of the resulting $k_\mathrm{T}$ and $z$ in the shower.

Figure 5.1 shows a comparison between the pure NLL predictions and those where this constraint has been implemented. The additional contribution of this is a power correction, that is formally not relevant for logarithmic resummation. The effect on the cumulative distributions is moderate, about 5% in the medium and low-$v$ region.

In addition, the effect of choosing the scale in the collinear term to be $k_T^2$ is investigated. This alters the slope of the thrust and $\mathrm{BKS}_{1/2}$ distributions in the small-$v$ region, due to additional sub-leading logarithmic terms in $R(v)$. This second setup corresponds to the first emission of a traditional parton shower, although formally none of the two is preferred over the other. It has no effect in the fractional energy observable, as for $x = 1$ the shower is ordered in $\xi = k_\mathrm{T}^2$ already.

The upper bound $z_{\max}$ is generally weaker than the constraint arising from the condition $\eta > 0$, listed in Table 3.1, that is needed in the soft term to remove soft double counting as described in Section 3.1.1. Figure 5.1 displays the additional effect on the NLL prediction when this constraint is applied in form of $z^{max}_{\lessgtr v,coll}$ as used in typical parton showers (see Equation (3.10)). The effects are about 10% on all observables, and they lower the prediction for $\Sigma(v)$ due to an increased branching probability.

Again, the effect of choosing the scale in the collinear term to be $k_T^2$ is investigated, which generates the same slope differences at small $v$ observed before. The effects are presented here in distributions calculated from only one emission, as they only influence the first emission properties. They are of course still present, and of the same size, if the distributions shown here are multiplied by the multiple emission function $\mathcal{F}(v)$ or a similar expression that emerges from the shower.

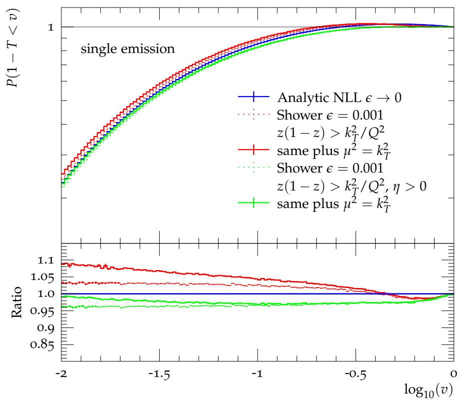


(a) Thrust

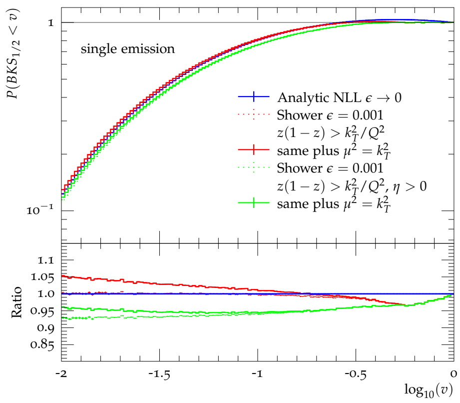


(b) $\mathrm{BKS}_{1/2}$

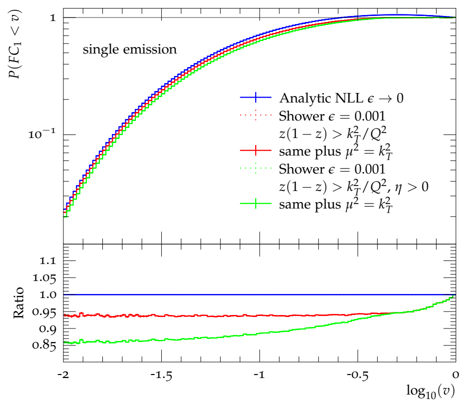


(c) $\mathrm{FC}_1$

Figure 5.1: Effects arising from momentum-conservation in the anti-collinear direction and from phase-space sectorization (removal of soft double counting in typical parton-shower implementations). Both are effects at the single-emission level, impacting terms in $R(v)$, see Table 3.1.

### 5.1.2 Multiple emission level

On the level of multiple emissions, several effects come into play. This is because the function $R'(v)$ that contains the $\alpha_s L$ dependence of the multiple emissions function $\mathcal{F}(v)$ is already single logarithmic, while a typical parton shower algorithm would not change the accuracy at which further terms are calculated. This adds many terms of higher logarithmic accuracy in the shower, via higher loop corrections in the running coupling but also through different phase space constraints.

Since introducing this into the shower also introduces a new weight depending on the value of $v$ at which one wants to compute $\Sigma(v)$, and hence the observable one considers, it is also not a preferable to eliminate these contributions in the advanced parton showers used in fully fledged Monte Carlo simulations. It is however important to be aware of the sizes of these contributions when comparing partons showers to each other and to analytic calculations.

In contrast to the power corrections of the previous section, most of the contributions shown here correspond to terms that actually appear for example at NNLL accuracy, i.e. when taking into account terms which are suppressed by a factor $1/L$ with respect to the NLL terms discussed here. They might thus be resolved by considering calculations and showers at a higher accuracy.

#### Integration limits

First the effect of lifting the restriction on the $z$ integration in the calculation of $\mathcal{F}(v)$ is investigated. This means to remove the constraint $z < 1 - v^{1/a}$ if $\xi < Q^2 v^{2/(a+b)}$ and replacing it by the constraint $\eta > 0$. This is, all emissions that are kinematically allowed are possible, although some of them are expected to be irrelevant in a NLL calculation.

In this case $R'(v)$ must be computed down to very small scales and it becomes mandatory to introduce an additional cutoff, as one would otherwise need to evaluate $\alpha_s$ at values where perturbation theory is no longer valid. It is to some extend arbitrary how such a cutoff is to be implemented. Here, this is done by adding the requirement $k_T^{min} = 0.5$ GeV.

The difference to the pure NLL result is shown in Figure 5.2. Independent of the observable, this change is one of the largest differences observed in this study. The large relative difference between the pure NLL result and the modified prediction at small $v$ shows that sub-leading logarithmic effects become important. This is expected anyway, however it can be seen that this happens well within the region that is measured at experiments and thus phenomenologically relevant.

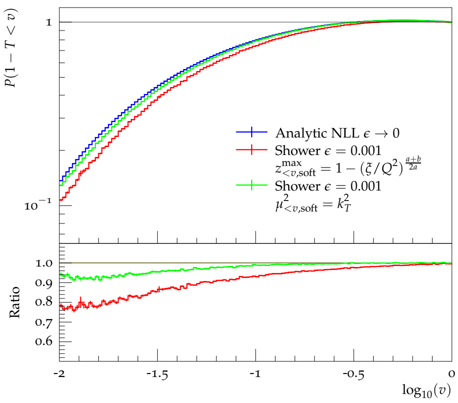


(a) Thrust

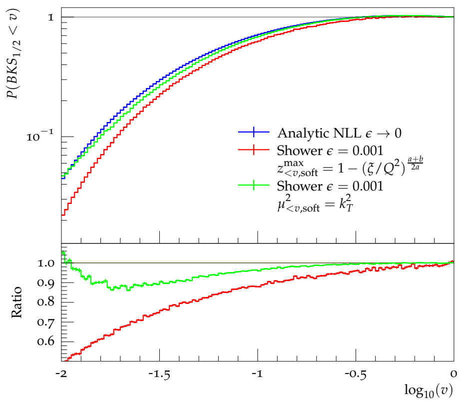


(b) $\mathrm{BKS}_{1/2}$

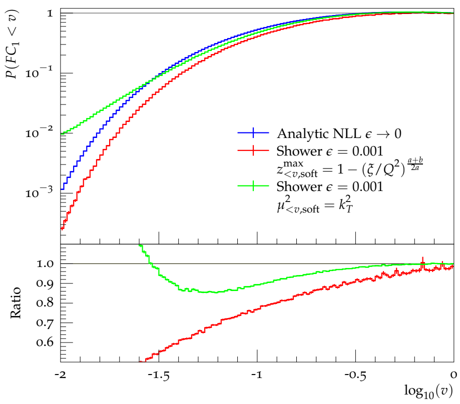


(c) $\mathrm{FC}_1$

Figure 5.2: Effect of replacing the constraint $z < 1 - v^{1/a}$ for $\xi < Q^2 v^{2/(a+b)}$ by the phase-space sectorization constraint, $\eta > 0$ and effects arising from the evaluation of the strong coupling at $k_\mathrm{T}^2$ with $k_\mathrm{T}^\mathrm{min} = 0.5$ GeV.

Next, the effect originating in the evaluation of the running coupling at $Q^2 v^{2/(a+b)}(1-z)^{2b/(a+b)}$ if $\xi < Q^2 v^{2/(a+b)}$ is studied. Again the constraint $k_T^{min} = 0.5\ GeV$ needs to be implemented, in order to deal with the QCD Landau pole and to stay in the range of validity of perturbation theory.

Figure 5.2 shows that the predictions for all observables exhibit relatively large changes. They also show convergence issues at small values, which arise from the lower cutoff in $k_T$. This effect is most pronounced in $\mathrm{FC}_1$, where it starts to appear around $10^{-1.5}$. Note, however, that practical measurements of $\mathrm{FC}_1$ would be impacted by non-perturbative corrections in this regime. The problem is therefore purely academic in nature, hence no attempt at a solution is done here.

## The CMW scheme and $\alpha_s$ at two loop accuracy

Formally the CMW scheme is the key to achieving NLL accuracy in a parton shower for the observables considered here [77], as it provides the additional terms $\propto K$ in Equation (3.32). The numerical impact on $R(v)$ is investigated in Figure 5.3. There is a noticeable impact, largest for $FC_1$ and at small $v$. This shows that the corresponding terms are also numerically important to achieve a result that resembles NLL accurate calculations.

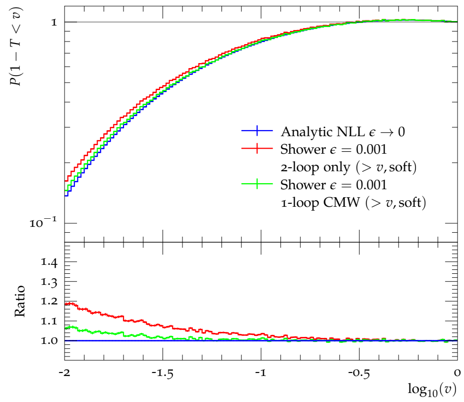


(a) Thrust

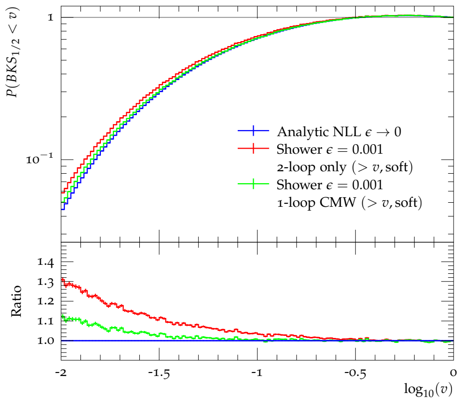


(b) $\mathrm{BKS}_{1/2}$

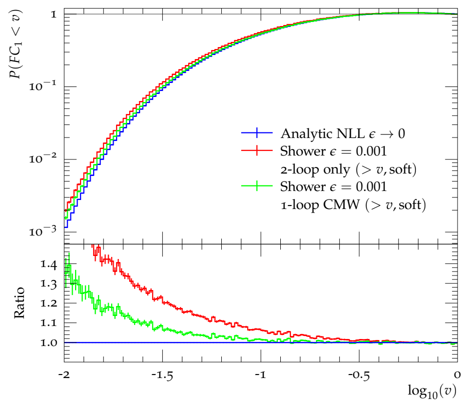


(c) $\mathrm{FC}_1$

Figure 5.3: Effects of replacing 2-loop CMW running of $\alpha_s$ in the leading terms of the NLL result. The red line is computed without the CMW scheme, while the green line is computed by using the CMW scheme at 1-loop.

Figure 5.4 displays the effect of replacing 1-loop by 2-loop running couplings and of using the CMW scheme in sub-leading terms of the NLL calculation (see Table 3.1). The red line is computed by making the replacements only in the soft-enhanced part of the splitting function for $\xi < Q^2 v^{2/(a+b)}$, and the red dotted line corresponds to not using the CMW scheme if $\xi < Q^2 v^{2/(a+b)}$.

It is evident that the effects are sizeable over most of the observable range, and most pronounced at small $v$. The use of the CMW scheme has the biggest impact. Note in particular that not using the CMW scheme in the computation of $\mathcal{F}(v)$ has nearly the same impact as not using the CMW scheme in the computation of $R(v)$.

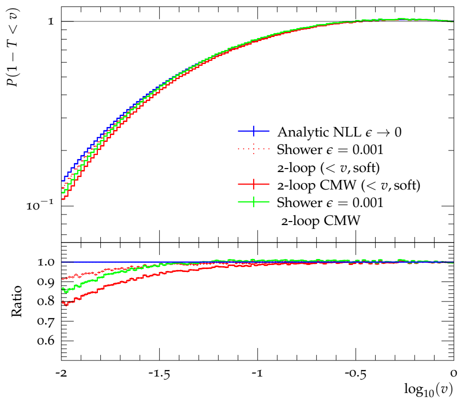


(a) Thrust

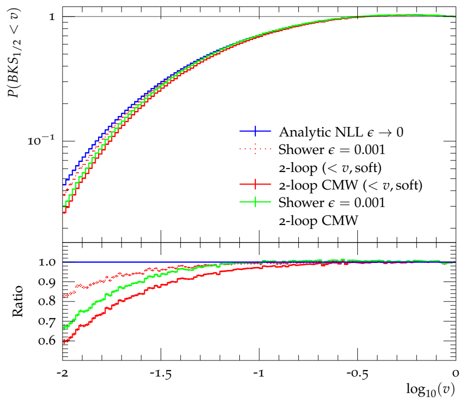


(b) $\mathrm{BKS}_{1/2}$

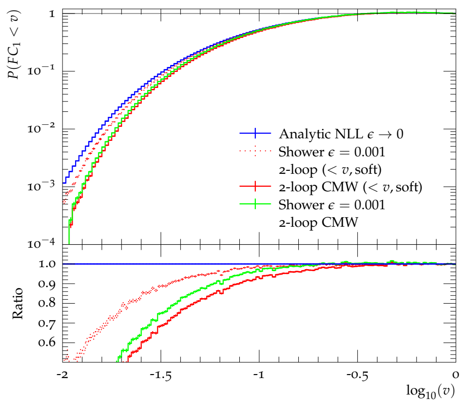


(c) $\mathrm{FC}_1$

Figure 5.4: Effects of replacing 1-loop by 2-loop CMW running of $\alpha_s$ in the subleading terms of the NLL result. The red line is computed by making the replacements only in the soft-enhanced term if $\xi < Q^2 v^{2/(a+b)}$, the red dotted line corresponds to not using the CMW scheme in this region.

### 5.1.3 Pure NLL resummation and default parton shower

Figure 5.5 shows the cumulative effect of all changes discussed so far. In addition results from a simulation where the observable is computed using its definition in terms of four-momenta, Equations (2.18), (2.19) and (2.20) for the observables used here, rather than using the soft approximation in Equation (2.17), are presented.

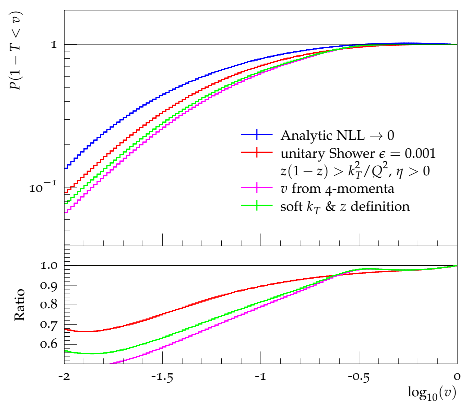


(a) Thrust

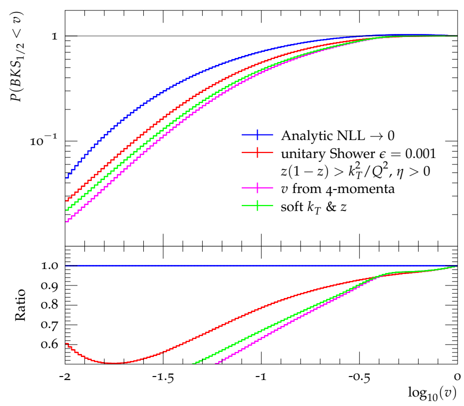


(b) $\mathrm{BKS}_{1/2}$

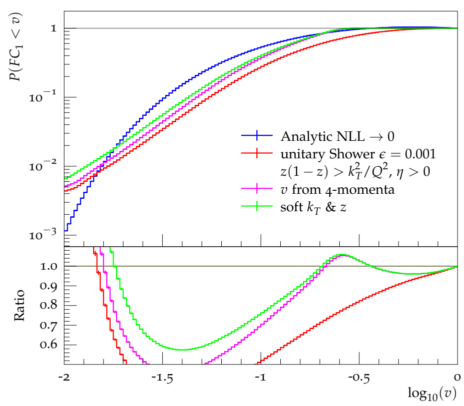


(c) $\mathrm{FC}_1$

Figure 5.5: Comparison of pure NLL resummation and plain DGLAP parton shower, effects of approximating the observable compared to exact calculation using four-momenta and evolution in dipole-$k_T$.

In this context it becomes important to take into account the effect that emissions away from the strict soft limit inevitably change the momenta of the hard partons. Subsequent emissions are then computed based on the momenta of the quark lines with recoil effects taken into account. This can have a significant impact on the result, depending on the precise definition of the transverse momentum and momentum fraction away from the soft and collinear limit.

The magenta line in Figure 5.5 corresponds to the conventions of [112], while the green line corresponds to the conventions of [39]. In the latter case the transverse momentum coincides with Equation (2.5) of [33].[1] Note that the phase-space sectorization constraint, $\eta > 0$, generates a different restriction on $z$ once recoil is taken into account, and that this condition depends on the choice of evolution and splitting variable.

## 5.2 Modern dipole showers

This section presents a comparison of the previous results with predictions from a dipole-like parton shower. As described in Section 3.1.2, in such parton showers the soft enhanced part of the collinear splitting function is typically replaced by a partial fraction of the soft eikonal matched to the collinear limit [116, 112]. At the same time, the phase-space sectorization is removed, i.e. the restriction $\eta > 0$ is lifted.

A complete description of the parton-shower algorithm employed here can be found in [39]. In short, the splitting functions of Section 3.1.2, Equation (3.16) are used. The integration limits are defined by momentum conservation. Apart from that the integration is performed over the whole range. The strong coupling constant is evaluated at two loops in the CMW scheme. According to the phase space factorisation in [112], where also the splitting functions are initially derived, a corresponding Jacobian is included.

Figure 5.6 shows a comparison between results from the dipole-like parton shower in its default configuration (including gluon splitting) and from a modified version, tailored to match the settings of the parton shower used in Section 5.1.3, Figure 5.5. It is interesting to observe that the dipole-shower prediction lies between the parton-shower result and the analytic result for all observables, and in the case of thrust agrees very well with the analytic prediction. In the measurable range at LEP energies, the predictions for $\mathrm{FC}_1$ also agree fairly well between the dipole-shower and the analytic result.

[1] Note that the constraint $z(1-z) > k_T^2/Q^2$ arising from minus momentum conservation applies to this definition in the case of final-state emitter with final-state spectator, such that the results in Figure 5.1 remain valid.

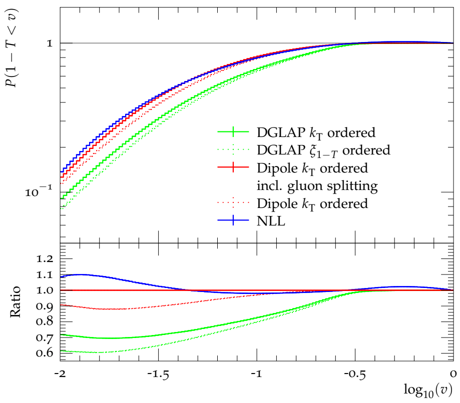


(a) Thrust

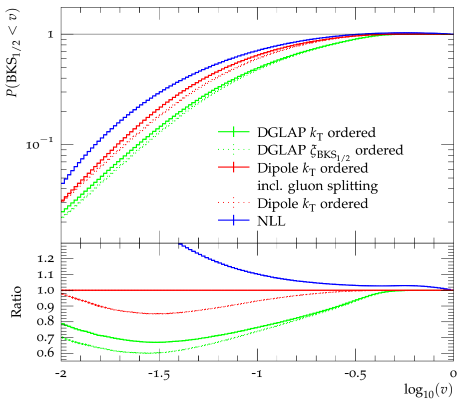


(b) $\mathrm{BKS}_{1/2}$

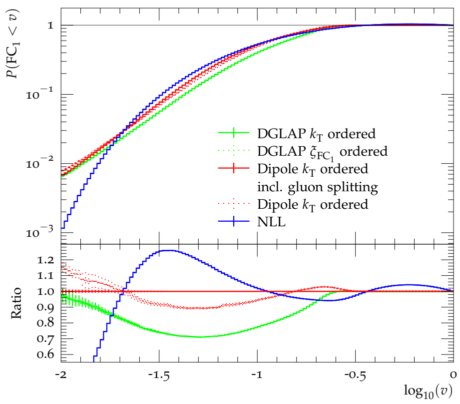


(c) $\mathrm{FC}_1$

Figure 5.6: Comparison between plain DGLAP parton shower ordered in $\xi$ to DGLAP parton shower ordered in dipole-$k_T$ and dipole shower with and without gluon splitting. The blue line shows the analytic NLL result as a reference.

# 6 Conclusions

In the study presented here, a detailed comparison between pure NLL resummation and parton showers has been performed for additive three-jet observables in $e^+e^-$ annihilation to hadrons.

The effects can broadly be classified as related to probability or momentum conservation. While different treatments of these effects lead to formally subleading corrections to the resummed distributions, it can have a sizeable impact, in particular also in the region where measurements are usually performed and which is thus of phenomenological interest.

The effects of momentum conservation at single emission level have been found to contribute a rather moderate correction to the pure NLL result, which are partially cancelled by corresponding choices of the scale of $\alpha_s$ at least for some observables. It has been shown that further restricting the available phase space, for example to avoid negative weights, has an impact of similar size, though not necessarily in the same direction so that these contributions can also partially cancel each other. It should be noted that these are differences that arise in any approach to soft gluon resummation that neglects power suppressed contributions. Even if the effect is found to be moderate here, it might become a dominating difference if resummation and shower would operate at a higher logarithmic accuracy. Work towards a formalism taking into account these types of corrections analytically has been done in different frameworks [117, 118]. No generally accepted result appears to have emerged so far, however, at least not to the extend of a numerical calculation of these effects.

The largest effect found here is the difference that arises when the phase space restriction of the soft term for multiple emissions is calculated only from momentum conservation rather than from formal considerations in the computation of the multiple emission function $\mathcal{F}$.

Also large changes are found when the strong coupling is evaluated at the scale $k_\mathrm{T}$ of the actual splitting, rather than at the generic scale corresponding to $v$ that is used in the analytic calculation of $\mathcal{F}$. The last two points correspond to corrections to $\mathcal{F}$ that are relevant at higher logarithmic accuracy. Thus they are expected to be partially resolved at NNLL accuracy.

The effects associated to the specific treatment of the strong coupling constant were evaluated. It is found that the use of the CMW scheme has a large impact, and is important to achieve results comparable to the NLL result. It is however noticed, that the use of the CMW scheme and terms corresponding to the running of $\alpha_s$ at two loop in regions where it is not necessary to achieve the accuracy aimed for introduces a correction of similar size, although this is formally a subleading effect.

These differences already have a large effect. However, the final step of actually constructing full events during the shower evolution and calculating the observable from this final state is a further effect of similar size. There is some dependence on the definition of the shower variables away from the exact soft and collinear limit. This choice is also subleading but has a noticeable effect.

Finally, a comparison to a modern dipole shower variant was performed. Interestingly enough, the results are in many cases considerably closer to the analytic result, at least in the range of applicability. However, the general statement about the sizes of the corrections remains.

In particular, since there is no formal preference for one of the variants, the differences found here are to be interpreted as a systematic uncertainty that is to be expected whenever a comparison between resummed calculations in an analytic framework and a parton shower is performed.

It has been shown that the differences can be assessed quantitatively by casting analytic resummation into a Markovian Monte-Carlo simulation and introducing momentum and probability conservation. Conversely, parton showers can be modified to violate momentum and probability conservation to reproduce pure NLL results. From a practical point of view this approach is disfavoured, as it leads to numerically inefficient Monte-Carlo algorithms.

# Bibliography

[1] S. Höche, D. Reichelt and F. Siegert, *Momentum conservation and unitarity in parton showers and NLL resummation*, `arXiv:1711.03497` [hep-ph].

[2] K. Kahle, *LHC reaches 2017 targets ahead of schedule*, Oct 2017, Accessed: 30.11.2017.

[3] M. Mangano (Ed.), *Physics at the FCC-hh, a 100 TeV pp collider*, vol. 3, CERN Yellow Reports: Monographs, 2017, `arXiv:1710.06353` [hep-ph].

[4] T. Behnke, J. E. Brau, B. Foster, J. Fuster, M. Harrison, J. M. Paterson, M. Peskin, M. Stanitzki, N. Walker and H. Yamamoto (Eds.), *The International Linear Collider Technical Design Report - Volume 1: Executive Summary*, 2013, `arXiv:1306.6327` [physics.acc-ph].

[5] F. Zimmermann et al., *FCC-ee Overview*, Proceedings, 55th ICFA Advanced Beam Dynamics Workshop on High Luminosity Circular $e^+e^-$ Colliders - Higgs Factory (HF2014): Beijing, China, October 9-12, 2014, 2015.

[6] M. Benedikt and F. Zimmermann, *Status of the Future Circular Collider Study*, 25th Russian Particle Accelerator Conference (RuPAC 2016) Saint Petersburg, Russia, November 21-25, 2016, 2016.

[7] T. Gleisberg, S. Höche, F. Krauss, A. Schälicke, S. Schumann and J. Winter, *Sherpa 1.$\alpha$, a proof-of-concept version*, JHEP **02** (2004), 056, [ `hep-ph/0311263`].

[8] T. Gleisberg, S. Höche, F. Krauss, M. Schönherr, S. Schumann, F. Siegert and J. Winter, *Event generation with Sherpa 1.1*, JHEP **02** (2009), 007, [ `arXiv:0811.4622` [hep-ph]].

[9] M. Bähr et al., *Herwig++ Physics and Manual*, Eur. Phys. J. **C58** (2008), 639–707, [ `arXiv:0803.0883` [hep-ph]].

[10] J. Bellm et al., *Herwig 7.0/Herwig++ 3.0 release note*, Eur. Phys. J. **C76** (2016), no. 4, 196, [ `arXiv:1512.01178` [hep-ph]].

[11] T. Sjöstrand, L. Lönnblad, S. Mrenna and P. Skands, *PYTHIA 6.3 Physics and Manual*, `hep-ph/0308153`.

[12] T. Sjöstrand, S. Mrenna and P. Skands, *A brief introduction to PYTHIA 8.1*, Comput. Phys. Commun. **178** (2008), 852–867, [ `arXiv:0710.3820` [hep-ph]].

[13] A. Buckley et al., *General-purpose event generators for LHC physics*, Phys. Rept. **504** (2011), 145–233, [ `arXiv:1101.2599` [hep-ph]].

[14] S. Höche, *Introduction to parton-shower event generators*, Proceedings of TASI 2014, 2015, pp. 235–295.

[15] R. K. Ellis, W. J. Stirling and B. R. Webber, *QCD and collider physics*, ed. 1, vol. 8, Cambridge Monogr. Part. Phys. Nucl. Phys. Cosmol., 1996.

[16] Y. L. Dokshitzer, D. Diakonov and S. I. Troian, *Hard Processes in Quantum Chromodynamics*, Phys. Rept. **58** (1980), 269–395.

[17] G. Parisi and R. Petronzio, *Small transverse momentum distributions in hard processes*, Nucl. Phys. **B154** (1979), 427.

[18] J. C. Collins and D. E. Soper, *Back-to-back jets in QCD*, Nucl. Phys. **B193** (1981), 381.

[19] G. F. Sterman, *Summation of large corrections to short-distance hadronic cross sections*, Nucl. Phys. **B281** (1987), 310.

[20] S. Catani and L. Trentadue, *Resummation of the QCD perturbative series for hard processes*, Nucl. Phys. **B327** (1989), 323.

[21] S. Catani and L. Trentadue, *Comment on QCD exponentiation at large $x$*, Nucl. Phys. **B353** (1991), 183–186, CAVENDISH-HEP-90-12.

[22] S. Catani, L. Trentadue, G. Turnock and B. R. Webber, *Resummation of large logarithms in $e^+e^-$ event shape distributions*, Nucl. Phys. **B407** (1993), 3–42.

[23] S. Catani et al., *QCD*, 1999 CERN Workshop on SM physics (and more) at the LHC, 2000.

[24] G. Dissertori et al., *Determination of the strong coupling constant using matched NNLO+NLLA predictions for hadronic event shapes in $e^+e^-$ annihilations*, JHEP **08** (2009), 036, [ `arXiv:0906.3436` [hep-ph]].

[25] T. Gehrmann, M. Jaquier and G. Luisoni, *Hadronization effects in event shape moments*, Eur. Phys. J. **C67** (2010), 57–72, [ `arXiv:0911.2422` [hep-ph]].

[26] C. W. Bauer, D. Pirjol and I. W. Stewart, *Soft collinear factorization in effective field theory*, Phys.Rev. **D65** (2002), 054022, [ `hep-ph/0109045`].

[27] C. W. Bauer, S. Fleming, D. Pirjol, I. Z. Rothstein and I. W. Stewart, *Hard scattering factorization from effective field theory*, Phys.Rev. **D66** (2002), 014017, [ `hep-ph/0202088`].

[28] N. Kidonakis and G. F. Sterman, *Resummation for QCD hard scattering*, Nucl. Phys. **B505** (1997), 321–348, [ `hep-ph/9705234`].

[29] N. Kidonakis, G. Oderda and G. F. Sterman, *Evolution of color exchange in QCD hard scattering*, Nucl.Phys. **B531** (1998), 365–402, [ `hep-ph/9803241`].

[30] E. Laenen, G. Oderda and G. F. Sterman, *Resummation of threshold corrections for single particle inclusive cross-sections*, Phys. Lett. **B438** (1998), 173–183, [ `hep-ph/9806467`].

[31] R. Bonciani, S. Catani, M. L. Mangano and P. Nason, *Sudakov resummation of multiparton QCD cross sections*, Phys. Lett. **B575** (2003), 268–278, [ `hep-ph/0307035`].

[32] A. Banfi, G. Salam and G. Zanderighi, *Semi-numerical resummation of event shapes*, JHEP **01** (2002), 018, [ `hep-ph/0112156`].

[33] A. Banfi, G. P. Salam and G. Zanderighi, *Principles of general final-state resummation and automated implementation*, JHEP **03** (2005), 073, [ `hep-ph/0407286`].

[34] A. Banfi, H. McAslan, P. F. Monni and G. Zanderighi, *A general method for the resummation of event-shape distributions in $e^+e^-$ annihilation*, JHEP **05** (2015), 102, [ `arXiv:1412.2126` [hep-ph]].

[35] E. Gerwick, S. Höche, S. Marzani and S. Schumann, *Soft evolution of multi-jet final states*, JHEP **02** (2015), 106, [ `arXiv:1411.7325` [hep-ph]].

[36] P. Gras, S. Höche, D. Kar, A. Larkoski, L. Lönnblad, S. Plätzer, A. Siódmok, P. Skands, G. Soyez and J. Thaler, *Systematics of quark/gluon tagging*, JHEP **07** (2017), 091, [ `arXiv:1704.03878` [hep-ph]].

[37] S. Höche, F. Krauss and S. Prestel, *Implementing NLO DGLAP evolution in Parton Showers*, JHEP **10** (2017), 093, [ `arXiv:1705.00982` [hep-ph]].

[38] S. Schumann and F. Krauss, *A parton shower algorithm based on Catani-Seymour dipole factorisation*, JHEP **03** (2008), 038, [ `arXiv:0709.1027` [hep-ph]].

[39] S. Höche and S. Prestel, *The midpoint between dipole and parton showers*, Eur. Phys. J. **C75** (2015), no. 9, 461, [ `arXiv:1506.05057` [hep-ph]].

[40] S. Plätzer and S. Gieseke, *Coherent Parton Showers with Local Recoils*, JHEP **01** (2011), 024, [ `arXiv:0909.5593` [hep-ph]].

[41] S. Plätzer and M. Sjödahl, *Subleading $N_c$ improved Parton Showers*, JHEP **07** (2012), 042, [ `arXiv:1201.0260` [hep-ph]].

[42] Z. Nagy and D. E. Soper, *Parton shower evolution with subleading color*, JHEP **1206** (2012), 044, [ `arXiv:1202.4496` [hep-ph]].

[43] Y. L. Dokshitzer, V. A. Khoze, A. H. Mueller and S. I. Troyan, *Basics of perturbative QCD*, Gif-sur-Yvette, France: Ed. Frontieres, 1991.

[44] R. D. Field, *Applications of perturbative QCD*, Addison-Wesley, Redwood City, USA, 1989, Frontiers in physics, 77.

[45] J. Collins, *Foundations of perturbative QCD*, Cambridge University Press, 2013.

[46] T. Schörner-Sadenius (Ed.), *The Large Hadron Collider*, Springer, Berlin, 2015.

[47] G. W. Bennett et al., Muon g-2, *Measurement of the negative muon anomalous magnetic moment to 0.7 ppm*, Phys. Rev. Lett. **92** (2004), 161802, [ `arXiv:hep-ex/0401008` [hep-ex]].

[48] W. Altmannshofer, C. Niehoff, P. Stangl and D. M. Straub, *Status of the $B \to K^{*}\mu^{+}\mu^{-}$ anomaly after Moriond 2017*, Eur. Phys. J. **C77** (2017), no. 6, 377, [ `arXiv:1703.09189` [hep-ph]].

[49] A. D. Sakharov, *Violation of CP Invariance, c Asymmetry, and Baryon Asymmetry of the Universe*, Pisma Zh. Eksp. Teor. Fiz. **5** (1967), 32–35, [Usp. Fiz. Nauk161,61(1991)].

[50] S. P. Martin, *A Supersymmetry primer*, Adv. Ser. Direct. High Energy Phys. **21** (2010), 1–153, [ `arXiv:hep-ph/9709356` [hep-ph]], first published in Adv. Ser. Direct. High Energy Phys. **18** (1998), 1-98.

[51] F. Englert and R. Brout, *Broken Symmetry and the Mass of Gauge Vector Mesons*, Phys.Rev.Lett. **13** (1964), 321–323.

[52] P. W. Higgs, *Broken symmetries, massless particles and gauge fields*, Phys.Lett. **12** (1964), 132–133.

[53] P. W. Higgs, *Broken Symmetries and the Masses of Gauge Bosons*, Phys.Rev.Lett. **13** (1964), 508–509.

[54] G. Aad et al., ATLAS Collaboration, *Observation of a new particle in the search for the Standard Model Higgs boson with the ATLAS detector at the LHC*, Phys.Lett. **B716** (2012), 1–29, [ `arXiv:1207.7214` [hep-ex]].

[55] S. Chatrchyan et al., CMS Collaboration, *Observation of a new boson at a mass of 125 GeV with the CMS experiment at the LHC*, Phys.Lett. **B716** (2012), 30–61, [ `arXiv:1207.7235` [hep-ex]].

[56] S. Weinberg, *A Model of Leptons*, Phys. Rev. Lett. **19** (1967), 1264–1266.

[57] A. Salam, *Weak and Electromagnetic Interactions*, Conf. Proc. **C680519** (1968), 367–377.

[58] S. L. Glashow, *Partial Symmetries of Weak Interactions*, Nucl. Phys. **22** (1961), 579–588.

[59] R. P. Feynman, *Photon-hadron interactions*, Reading, MA, USA: Benjamin, 1972.

[60] J. D. Bjorken and E. A. Paschos, *Inelastic Electron Proton and gamma Proton Scattering, and the Structure of the Nucleon*, Phys. Rev. **185** (1969), 1975–1982, SLAC-PUB-0572.

[61] J. C. Collins, D. E. Soper and G. Sterman, *Factorization of hard processes in QCD*, Adv. Ser. Direct. High Energy Phys. **5** (1988), 1–91, [ `hep-ph/0409313`].

[62] B. Andersson, G. Gustafson, G. Ingelman and T. Sjöstrand, *Parton Fragmentation and String Dynamics*, Phys. Rept. **97** (1983), 31–145.

[63] T. Sjöstrand, *Jet Fragmentation of Nearby Partons*, Nucl.Phys. **B248** (1984), 469, DESY-T-84-01.

[64] B. R. Webber, *A QCD model for jet fragmentation including soft gluon interference*, Nucl. Phys. **B238** (1984), 492.

[65] S. Gieseke, C. Röhr and A. Siódmok, *Colour reconnections in Herwig++*, Eur. Phys. J. **C72** (2012), 2225, [ `arXiv:1206.0041` [hep-ph]].

[66] Y. L. Dokshitzer, G. Marchesini and B. Webber, *Dispersive approach to power-behaved contributions in QCD hard processes*, Nucl. Phys. **B469** (1996), 93–142, [ `arXiv:hep-ph/9512336` [hep-ph]].

[67] A. V. Manohar and M. B. Wise, *Power suppressed corrections to hadronic event shapes*, Phys. Lett. **B344** (1995), 407–412, [ `arXiv:hep-ph/9406392` [hep-ph]].

[68] G. P. Korchemsky and G. F. Sterman, *Nonperturbative corrections in resummed cross-sections*, Nucl. Phys. **B437** (1995), 415–432, [ `arXiv:hep-ph/9411211` [hep-ph]].

[69] G. P. Korchemsky, *Shape functions and power corrections to the event shapes*, Continuous advances in QCD. Proceedings, 3rd Workshop, QCD'98, Minneapolis, USA, April 16-19, 1998, 1998, [,489(1998)], pp. 489–498.

[70] E. Gardi and G. Grunberg, *Power corrections in the single dressed gluon approximation: The Average thrust as a case study*, JHEP **11** (1999), 016, [ `arXiv:hep-ph/9908458` [hep-ph]].

[71] A. H. Hoang and I. W. Stewart, *Designing gapped soft functions for jet production*, Phys. Lett. **B660** (2008), 483–493, [ `arXiv:0709.3519` [hep-ph]].

[72] T. Kinoshita, *Mass Singularities of Feynman Amplitudes*, J.Math.Phys. **3** (1962), 650–677.

[73] T. Lee and M. Nauenberg, *Degenerate Systems and Mass Singularities*, Phys. Rev. **133** (1964), B1549–B1562.

[74] F. Bloch and A. Nordsieck, *Note on the Radiation Field of the electron*, Phys. Rev. **52** (1937), 54–59.

[75] G. Aad et al., ATLAS, *Measurement of the inclusive jet cross section in pp collisions at* $\sqrt{s} = 2.76$ TeV *and comparison to the inclusive jet cross section at* $\sqrt{s} = 7$ TeV *using the ATLAS detector*, Eur. Phys. J. **C73** (2013), no. 8, 2509, [ arXiv:1304.4739 [hep-ex]].

[76] E. Zeidler, *Quantum Field Theory I: Basics in Mathematics and Physics: A Bridge Between Mathematicians and Physicists*, Springer, 2016.

[77] S. Catani, B. R. Webber and G. Marchesini, *QCD coherent branching and semiinclusive processes at large $x$*, Nucl. Phys. **B349** (1991), 635–654.

[78] W. A. Bardeen, A. J. Buras, D. W. Duke and T. Muta, *Deep Inelastic Scattering Beyond the Leading Order in Asymptotically Free Gauge Theories*, Phys. Rev. **D18** (1978), 3998, FERMILAB-PUB-78-042-THY, FERMILAB-PUB-78-042-T.

[79] D. J. Gross and F. Wilczek, *Ultraviolet Behavior of Nonabelian Gauge Theories*, Phys. Rev. Lett. **30** (1973), 1343–1346.

[80] H. D. Politzer, *Reliable Perturbative Results for Strong Interactions?*, Phys. Rev. Lett. **30** (1973), 1346–1349.

[81] C. Patrignani et al., Particle Data Group, *Review of Particle Physics*, Chin. Phys. **C40** (2016), no. 10, 100001.

[82] S. Schael et al., SLD Electroweak Group, DELPHI, ALEPH, SLD, SLD Heavy Flavour Group, OPAL, LEP Electroweak Working Group, L3, *Precision electroweak measurements on the Z resonance*, Phys. Rept. **427** (2006), 257–454, [ arXiv:hep-ex/0509008 [hep-ex]].

[83] C. Glasman, ZEUS, H1, *Precision measurements of alpha(s) at HERA*, J. Phys. Conf. Ser. **110** (2008), 022013, [ arXiv:0709.4426 [hep-ex]].

[84] G. Dissertori et al., *First determination of the strong coupling constant using NNLO predictions for hadronic event shapes in $e^+e^-$ annihilations*, JHEP **02** (2008), 040, [ arXiv:0712.0327 [hep-ph]].

[85] G. Dissertori et al., *Precise Determination of the Strong Coupling Constant at NNLO in QCD from the Three-Jet Rate in Electron–Positron Annihilation at LEP*, Phys. Rev. Lett. **104** (2010), 072002, [ arXiv:0910.4283 [hep-ph]].

[86] C. McNeile, C. T. H. Davies, E. Follana, K. Hornbostel and G. P. Lepage, *High-Precision c and b Masses, and QCD Coupling from Current-Current Correlators in Lattice and Continuum QCD*, Phys. Rev. **D82** (2010), 034512, [ arXiv:1004.4285 [hep-lat]].

[87] S. Perantonis and C. Michael, *Static potentials and hybrid mesons from pure SU(3) lattice gauge theory*, Nucl. Phys. **B347** (1990), 854–868, LTH-254.

[88] G. Bali and K. Schilling, *Static quark - anti-quark potential: Scaling behavior and finite size effects in SU(3) lattice gauge theory*, Phys.Rev. **D46** (1992), 2636–2646, WUB-92-02.

[89] S. Necco and R. Sommer, *The N(f) = 0 heavy quark potential from short to intermediate distances*, Nucl. Phys. **B622** (2002), 328–346, [ `arXiv:hep-lat/0108008` [hep-lat]].

[90] S. Jadach and M. Skrzypek, *Exact solutions of the QCD evolution equations using Monte Carlo method*, Acta Phys. Polon. **B35** (2004), 745–756, [ `arXiv:hep-ph/0312355` [hep-ph]].

[91] Y. I. Azimov, Y. L. Dokshitzer, V. A. Khoze and S. Troyan, *Similarity of Parton and Hadron Spectra in QCD Jets*, Z.Phys. **C27** (1985), 65–72, LENINGRAD-84-942.

[92] G. Zanderighi, `http://home.fnal.gov/~zanderi/Caesar/caesar.html`, Accessed: 26.11.2017.

[93] S. Catani, G. Turnock, B. Webber and L. Trentadue, *Thrust distribution in $e^+e^-$ annihilation*, Phys.Lett. **B263** (1991), 491–497, CAVENDISH-HEP-91-3.

[94] E. Farhi, *A QCD Test for Jets*, Phys. Rev. Lett. **39** (1977), 1587–1588, HUTP-77-A059.

[95] A. Heister et al., ALEPH, *Studies of QCD at $e^+e^-$ centre-of-mass energies between 91 and 209 GeV*, Eur. Phys. J. **C35** (2004), 457–486.

[96] P. Achard et al., L3, *Studies of hadronic event structure in $e^+e^-$ annihilation from* 30 GeV *to* 209 GeV *with the L3 detector*, Phys. Rept. **399** (2004), 71–174, [ `arXiv:hep-ex/0406049` [hep-ex]].

[97] P. Abreu et al., DELPHI, *Tuning and test of fragmentation models based on identified particles and precision event shape data*, Z. Phys. **C73** (1996), 11–60.

[98] G. Abbiendi et al., OPAL Collaboration, *Measurement of event shape distributions and moments in $e^+e^- \to$ hadrons at* 91 GeV - 209 GeV *and a determination of $\alpha_s$*, Eur.Phys.J. **C40** (2005), 287–316, [ `arXiv:hep-ex/0503051` [hep-ex]].

[99] C. F. Berger, T. Kucs and G. F. Sterman, *Interjet energy flow / event shape correlations*, Int. J. Mod. Phys. **A18** (2003), 4159–4168, [ `hep-ph/0212343`].

[100] C. F. Berger, T. Kucs and G. F. Sterman, *Event shape / energy flow correlations*, Phys. Rev. **D68** (2003), 014012, [ `hep-ph/0303051`].

[101] T. Sjöstrand and P. Z. Skands, *Transverse-momentum-ordered showers and interleaved multiple interactions*, Eur. Phys. J. **C39** (2005), 129–154, [ hep-ph/0408302].

[102] V. N. Gribov and L. N. Lipatov, *Deep inelastic e-p scattering in perturbation theory*, Sov. J. Nucl. Phys. **15** (1972), 438–450.

[103] L. N. Lipatov, *The parton model and perturbation theory*, Sov. J. Nucl. Phys. **20** (1975), 94–102.

[104] Y. L. Dokshitzer, *Calculation of the structure functions for deep inelastic scattering and $e^+e^-$ annihilation by perturbation theory in quantum chromodynamics*, Sov. Phys. JETP **46** (1977), 641–653.

[105] G. Altarelli and G. Parisi, *Asymptotic freedom in parton language*, Nucl. Phys. **B126** (1977), 298–318.

[106] D. Amati, A. Bassetto, M. Ciafaloni, G. Marchesini and G. Veneziano, *A treatment of hard processes sensitive to the infrared structure of QCD*, Nucl. Phys. **B173** (1980), 429.

[107] V. V. Sudakov, *Vertex parts at very high-energies in quantum electrodynamics*, Sov. Phys. JETP **3** (1956), 65–71.

[108] G. Marchesini and B. R. Webber, *Simulation of QCD Jets Including Soft Gluon Interference*, Nucl. Phys. **B238** (1984), 1.

[109] S. Höche, F. Krauss, M. Schönherr and F. Siegert, *A critical appraisal of NLO+PS matching methods*, JHEP **09** (2012), 049, [ arXiv:1111.1220 [hep-ph]].

[110] L. Lönnblad, *Fooling Around with the Sudakov Veto Algorithm*, Eur.Phys.J. **C73** (2013), 2350, [ arXiv:1211.7204 [hep-ph]].

[111] S. Plätzer and M. Sjödahl, *The Sudakov Veto Algorithm Reloaded*, Eur. Phys. J. Plus **127** (2012), 26, [ arXiv:1108.6180 [hep-ph]].

[112] S. Catani and M. H. Seymour, *A general algorithm for calculating jet cross sections in NLO QCD*, Nucl. Phys. **B485** (1997), 291–419, [ hep-ph/9605323].

[113] S. Catani, D. de Florian, M. Grazzini and P. Nason, *Soft-gluon resummation for Higgs boson production at hadron colliders*, JHEP **07** (2003), 028, [ hep-ph/0306211].

[114] G. Luisoni and S. Marzani, *QCD resummation for hadronic final states*, J. Phys. **G42** (2015), no. 10, 103101, [ arXiv:1505.04084 [hep-ph]].

[115] T. Sjöstrand, S. Mrenna and P. Skands, *PYTHIA 6.4 physics and manual*, JHEP **05** (2006), 026, [ hep-ph/0603175].

[116] R. Ellis, D. Ross and A. Terrano, *The Perturbative Calculation of Jet Structure in $e^+e^-$ Annihilation*, Nucl. Phys. **B178** (1981), 421.

[117] E. Laenen, G. Stavenga and C. D. White, *Path integral approach to eikonal and next-to-eikonal exponentiation*, JHEP **03** (2009), 054, [ arXiv:0811.2067 [hep-ph]].

[118] I. Feige, D. W. Kolodrubetz, I. Moult and I. W. Stewart, *A Complete Basis of Helicity Operators for Subleading Factorization*, JHEP **11** (2017), 142, [ arXiv:1703.03411 [hep-ph]].

# Acknowledgement/Danksagung

# Erklärung

Hiermit versichere ich, die vorliegende Arbeit ohne Benutzung anderer als der von mir angegebenen Quellen und Hilfsmittel und ohne unzulässige Hilfe dritter angefertigt zu haben. Alle aus fremden Quellen direkt oder indirekt übernommenen Gedanken sind als solche gekennzeichnet.

Die Arbeit wurde noch keiner Prüfungsbehörde in gleicher oder ähnlicher Form vorgelegt.

Dresden, 11.12.2017,

Daniel Reichelt